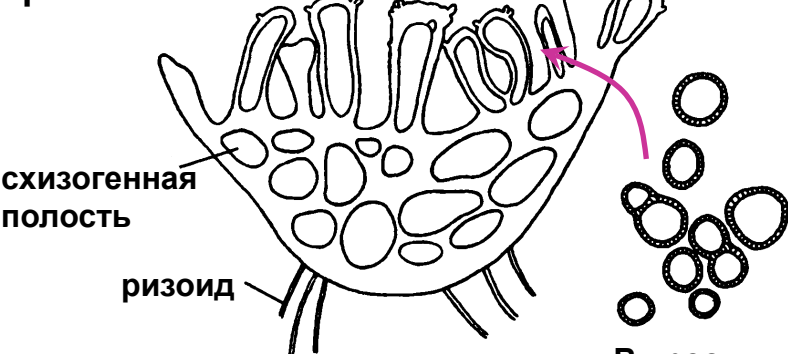


Phaeoceros laevis

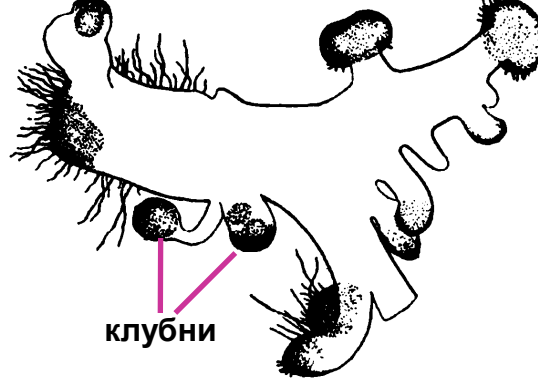
ОТДЕЛ
Anthocerotophyta

14 родов, 250 видов

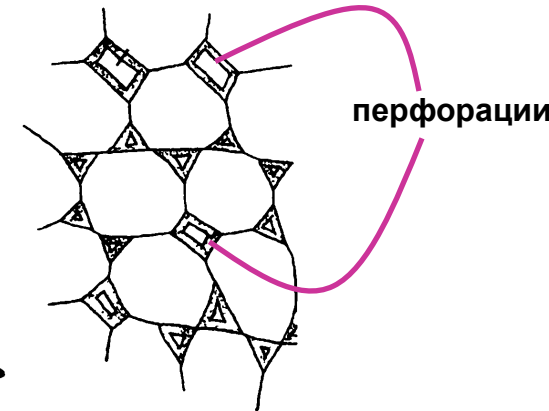
Folioceros appendiculaus, поперечный срез таллома



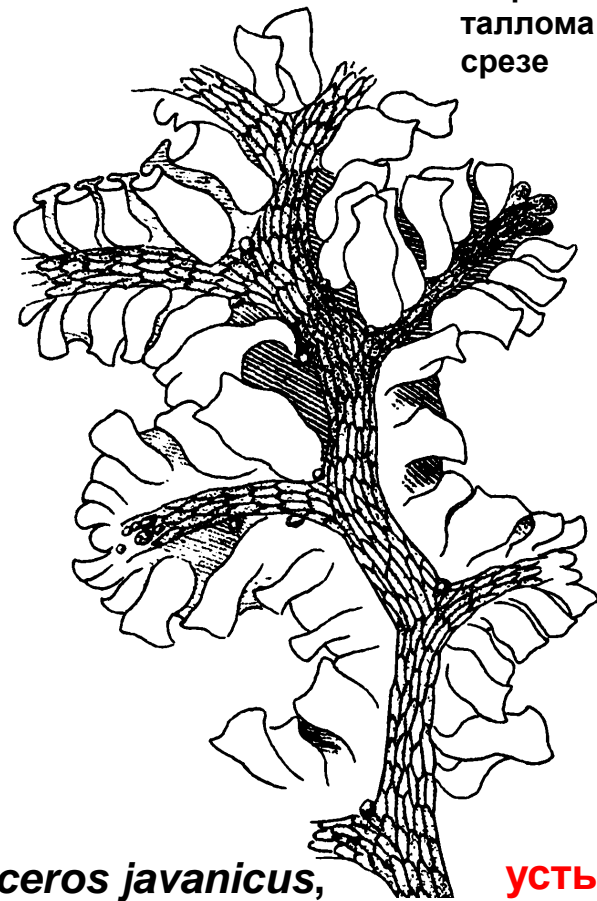
Phaeoceros bulbiculosus, вид таллома с дорзальной стороны



Dendroceros breutelii, однослойный край таллома



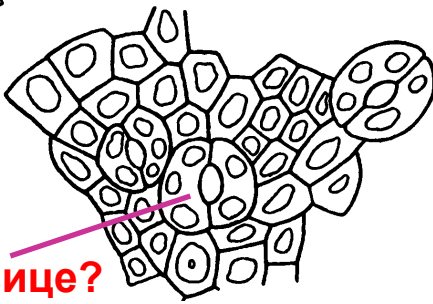
Выросты таллома на срезе



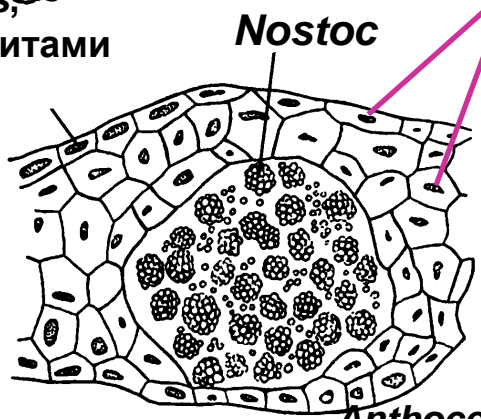
Nonothylas orbicularis, слоевище со спорофитами

1 пластида в каждой клетке

устыице?

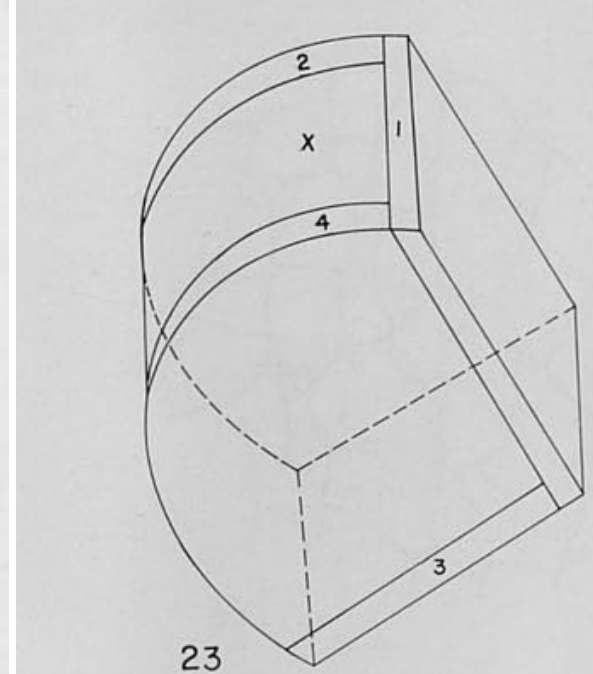
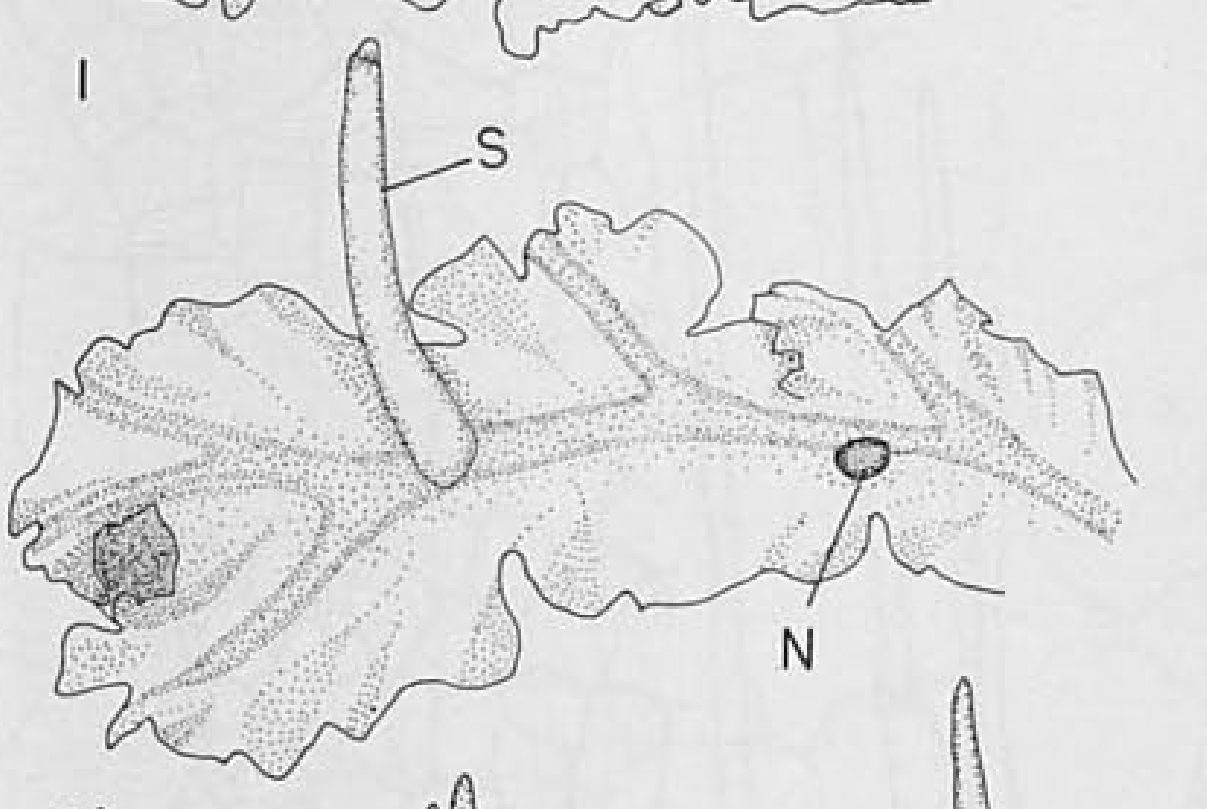


Dendroceros sp., брюшная эпидерма



Anthoceros agrestis, срез таллома

Dendroceros javanicus, таллом

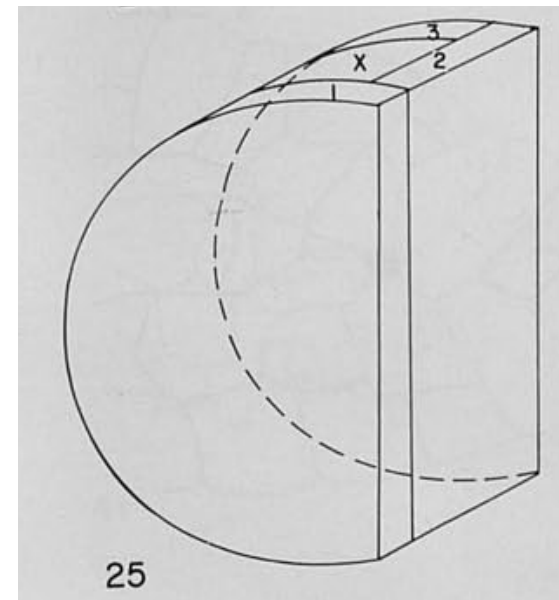


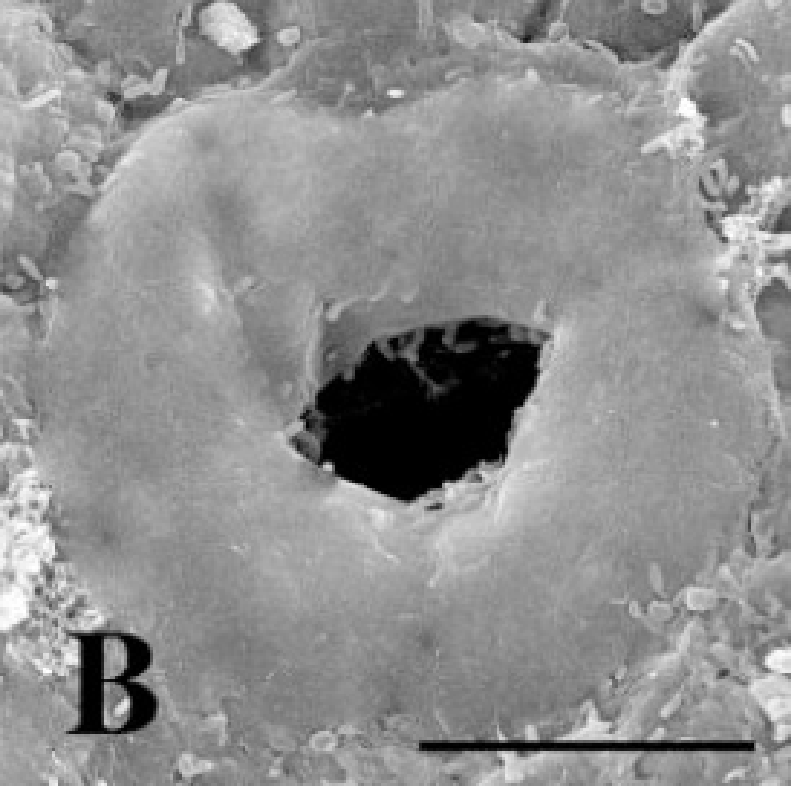
Клиновидная апикальная клетка (все кроме *Dendroceros*)

Dendroceros, дихтомическое ветвление

Дихтомическое ветвление установлено у гаметофитов всех изученных в этом отношении антоцеротовых и представляет собой оригинальную особенность этой группы

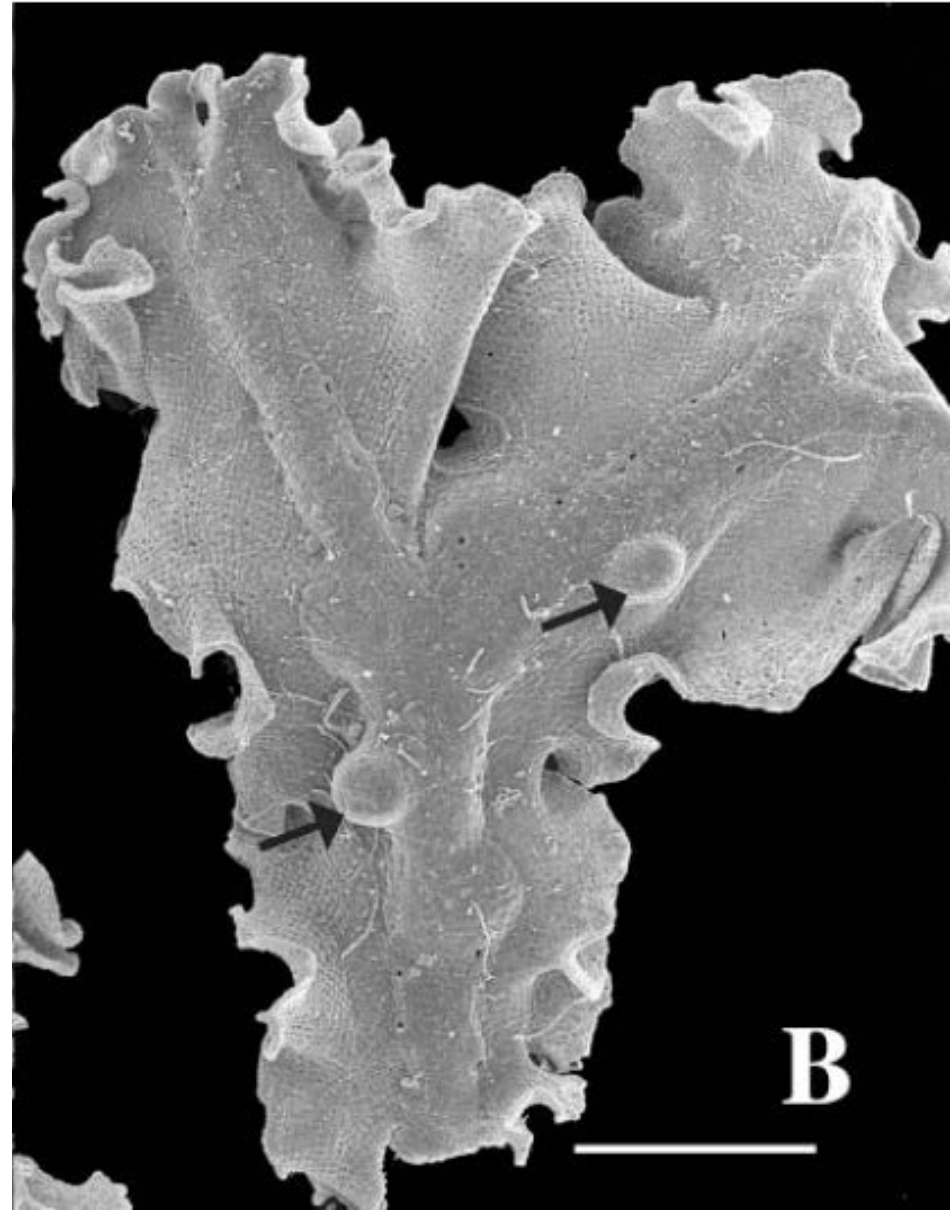
Полудисковидная апикальная клетка *Dendroceros*





открытое устье

Dendroceros crispatus: слоевище с нижней стороны

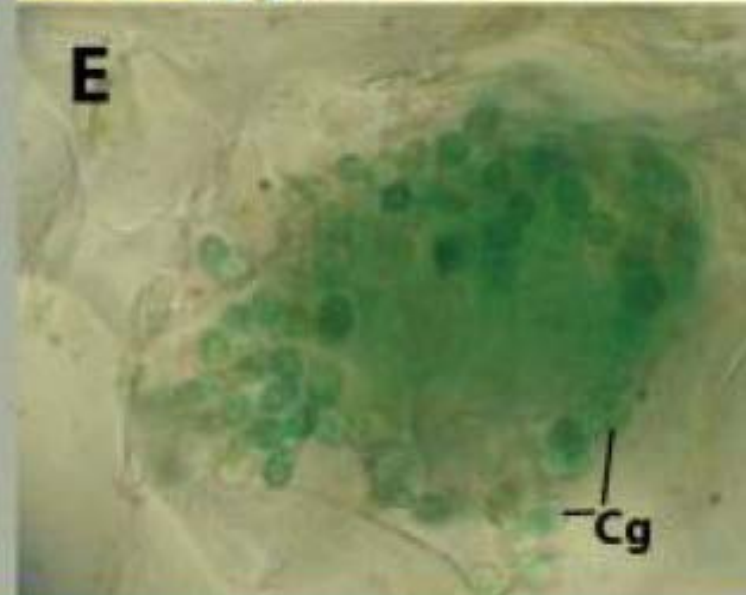
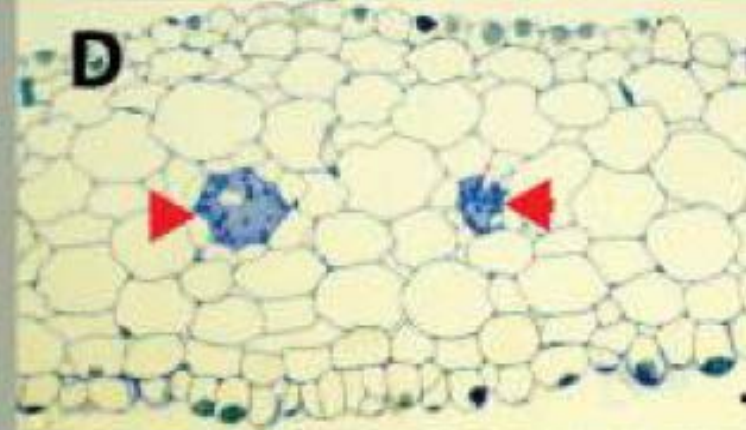
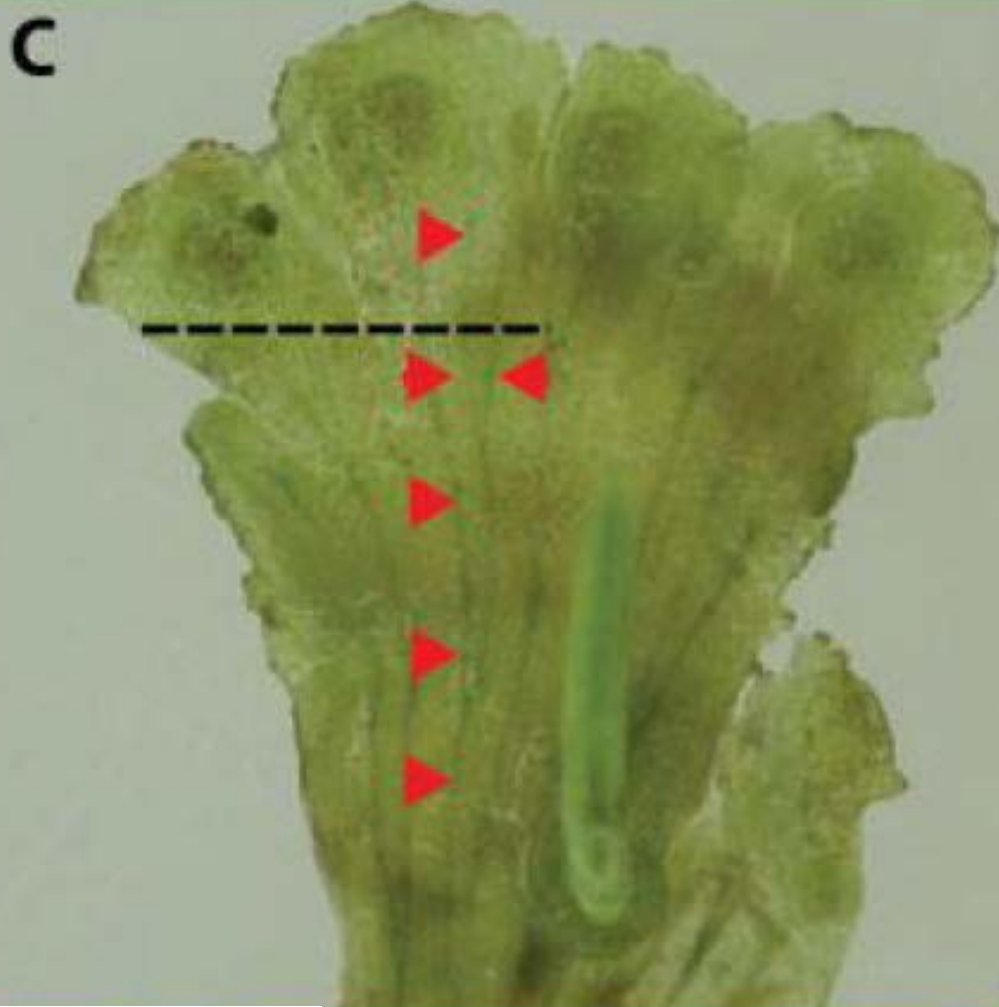


стрелки – колонии *Nostoc*

Folioceros dixitianus
Индия, Западные Гаты



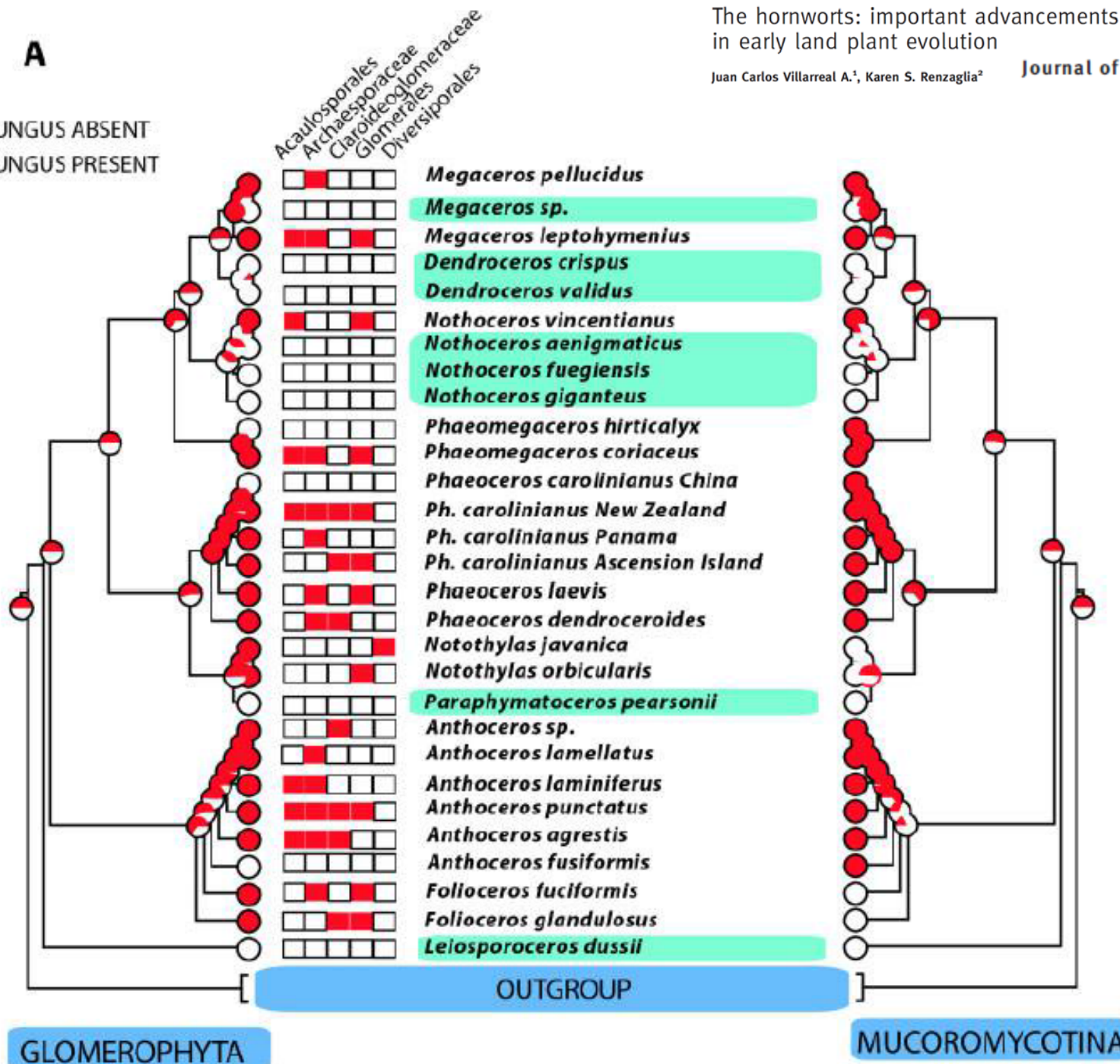
Колонии
Nostoc



(C) *Leiosporoceros dussii* (Steph.) Hässel. Bifurcating strands of *Nostoc* parallel the main axis of the thallus (red arrows) in a female plant with one sporophyte. A dashed line across represent the transverse section presented in Figure 4D, two opposite arrows represent the two individual strands in Figure 4D. Bar = 2 mm. (D) *Leiosporoceros dussii* (Steph.) Hässel. Transverse section of a mature thallus with two central *Nostoc* canals (red arrows) at the level of represented by dashed lines in Figure 4C. Bar = 75 μ m. (E) Higher magnification of a canal with *Nostoc* (blue-green filaments), note the abundant cyanophycian granules (Cg) in the individual cells (see Villarreal & Renzaglia, 2006 for ultrastructural features). Bar = 10 μ m.

Hornworts are arguably the oldest land plant lineage with a widespread symbiosis with cyanobacteria. Most hornwort species develop globose *Nostoc* colonies inside their thalli and multiple re-infections occur throughout their life span. The sole exception is *Leiosporoceros* that has bifurcating strands of *Nostoc* locked inside the thallus, potentially enhancing the transfer of metabolites between partners

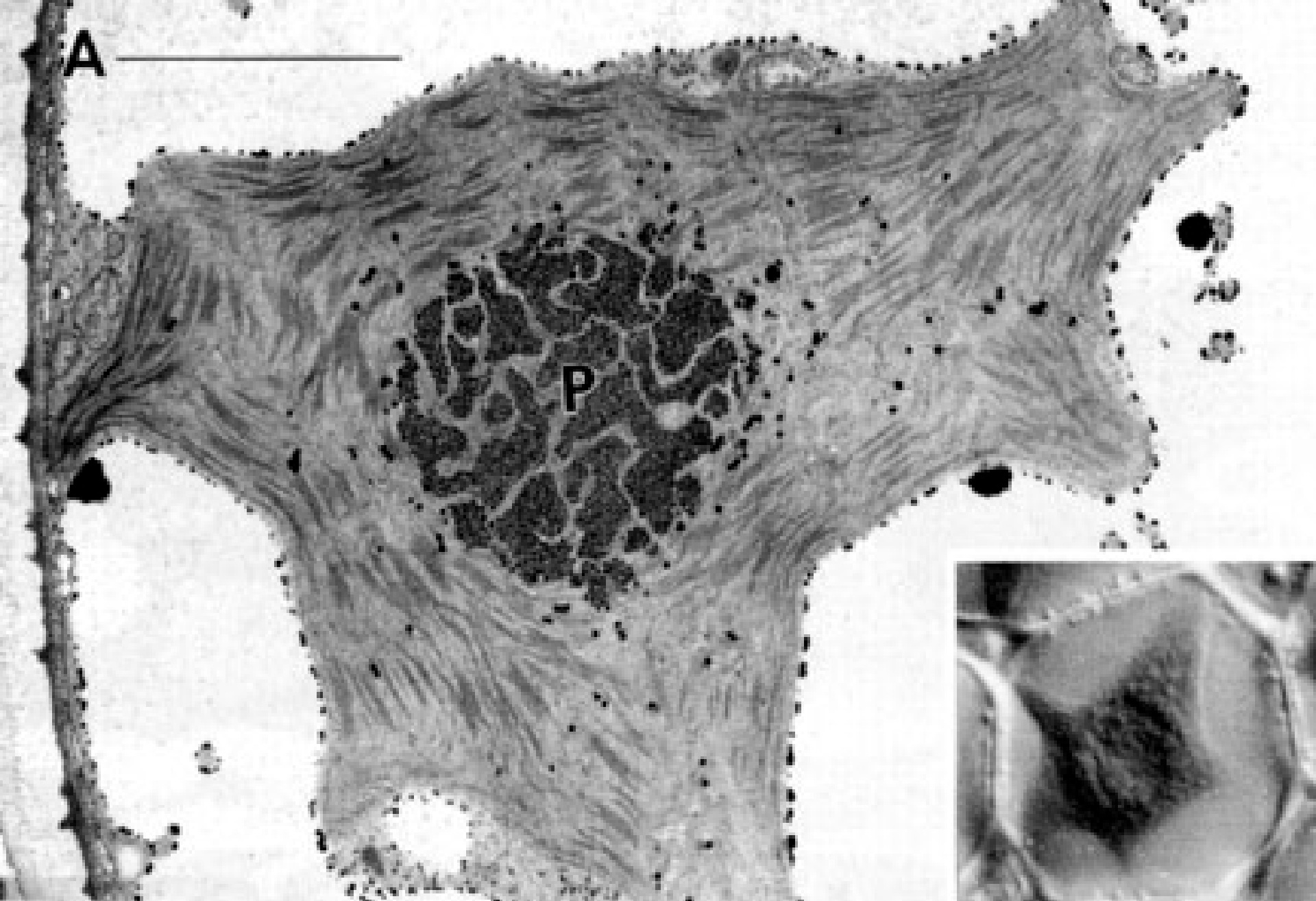
○ FUNGUS ABSENT
● FUNGUS PRESENT



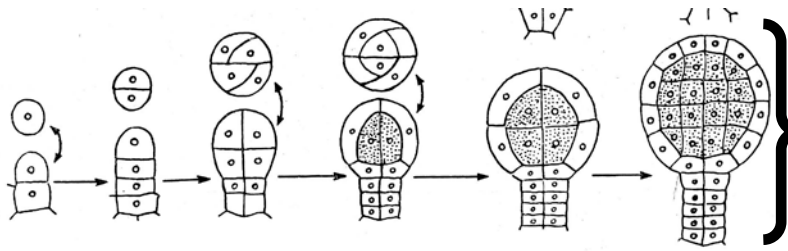
GLOMEROPHYTA

OUTGROUP

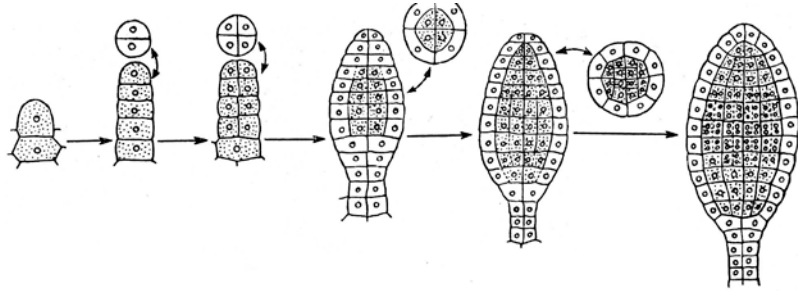
MUCOROMYCOTINA



Dendroceros tubercularis: хлоропласт с пиреноидом



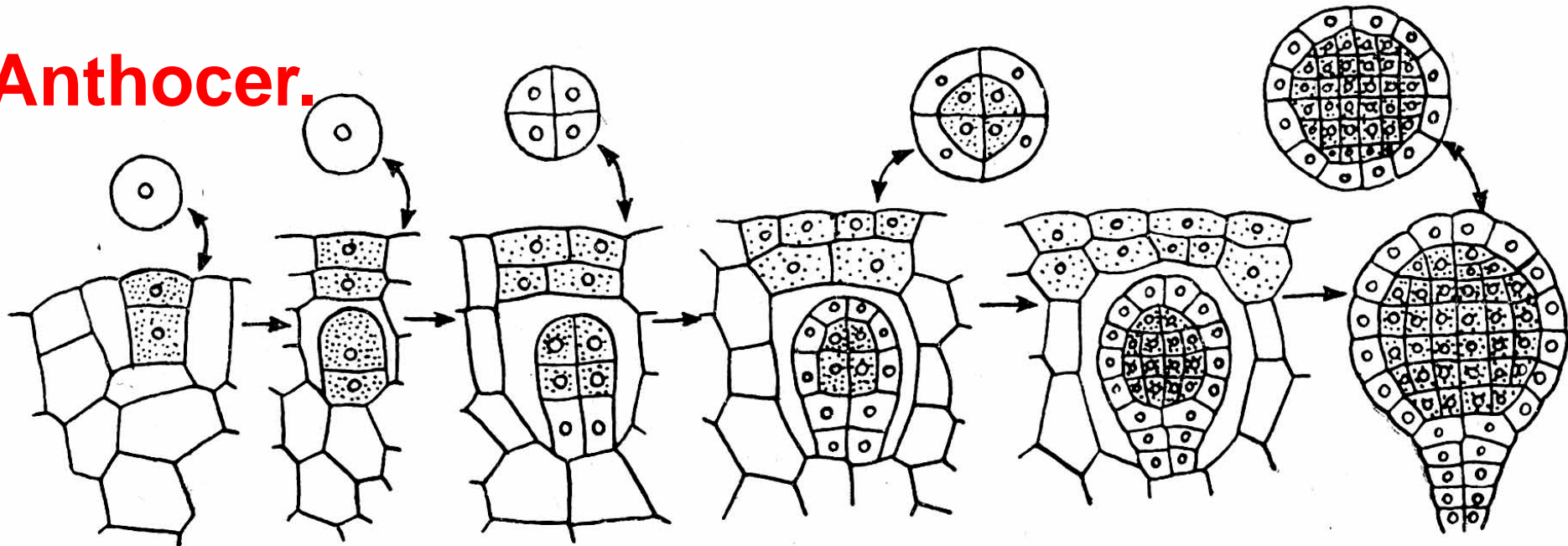
Jungermann.
Metzger.



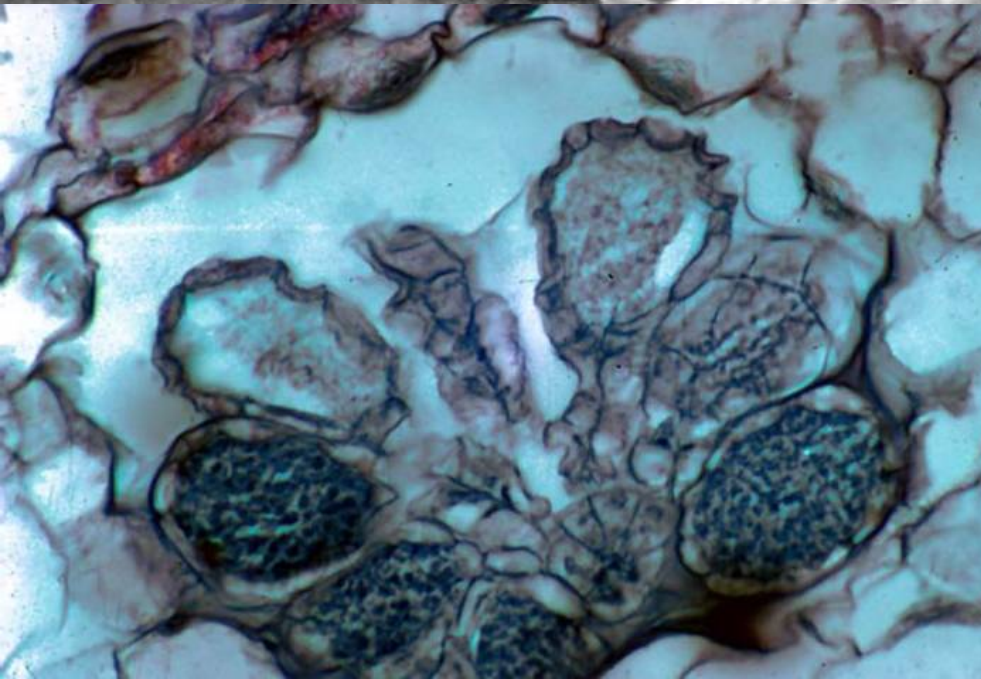
Marchant.

Развитие
антеридиев

Anthocer.



Dendroceros



Антеридии



Anthoceros

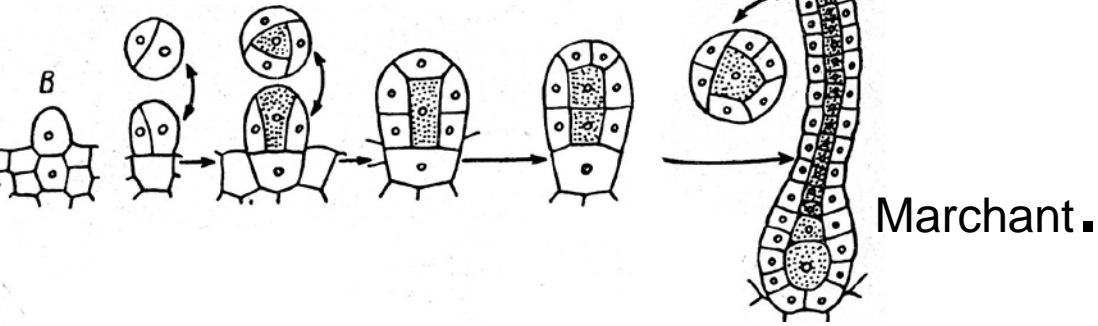
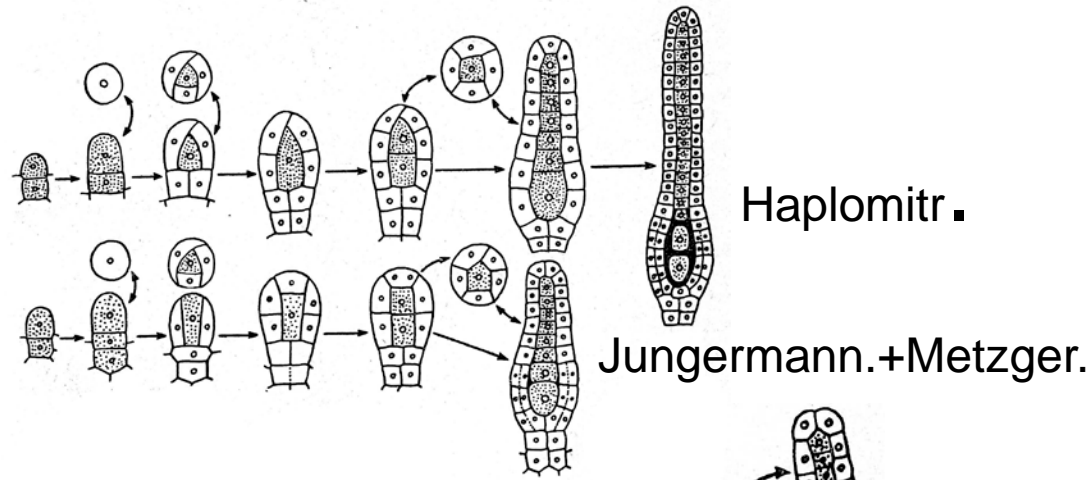


Foliosceros dixitianus
Индия, Западные Гаты

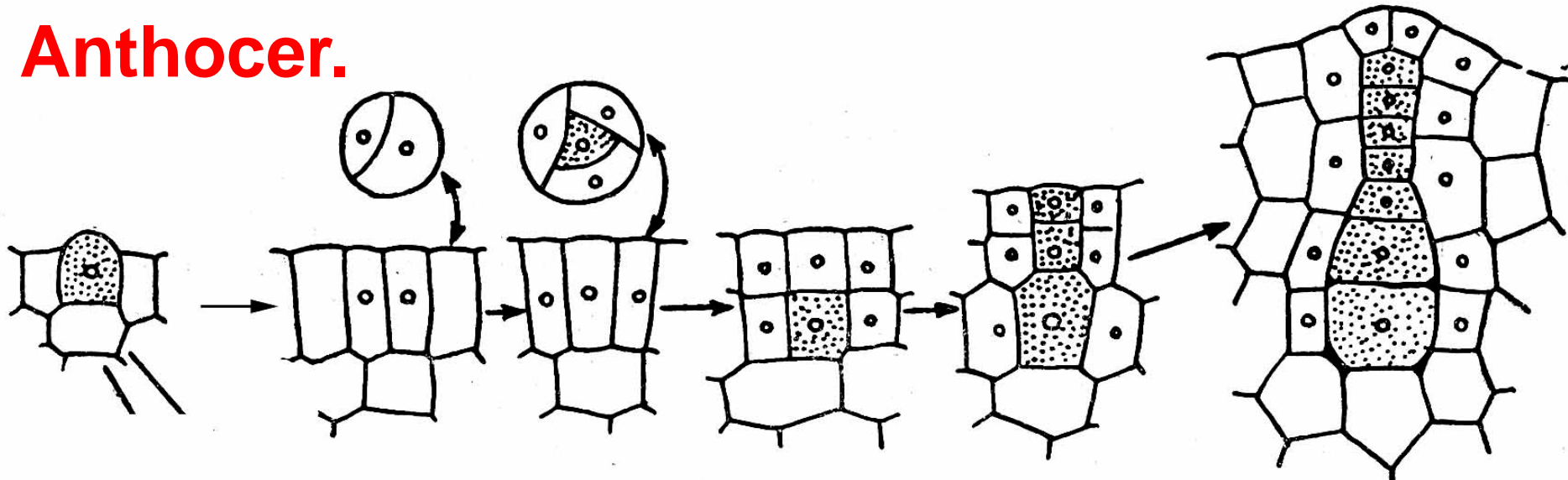
Folioceros dixitianus
Индия, Западные Гаты

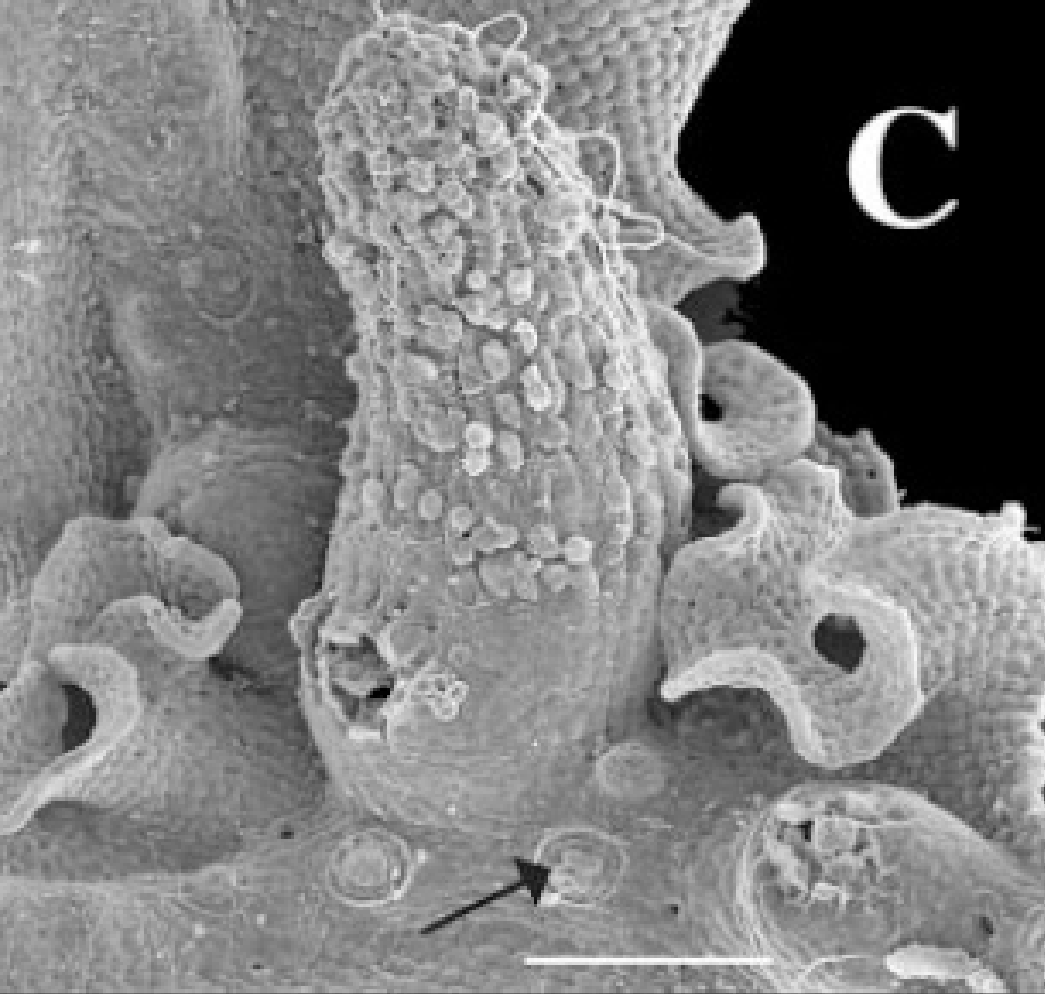


Развитие архегониев



Anthoceros.





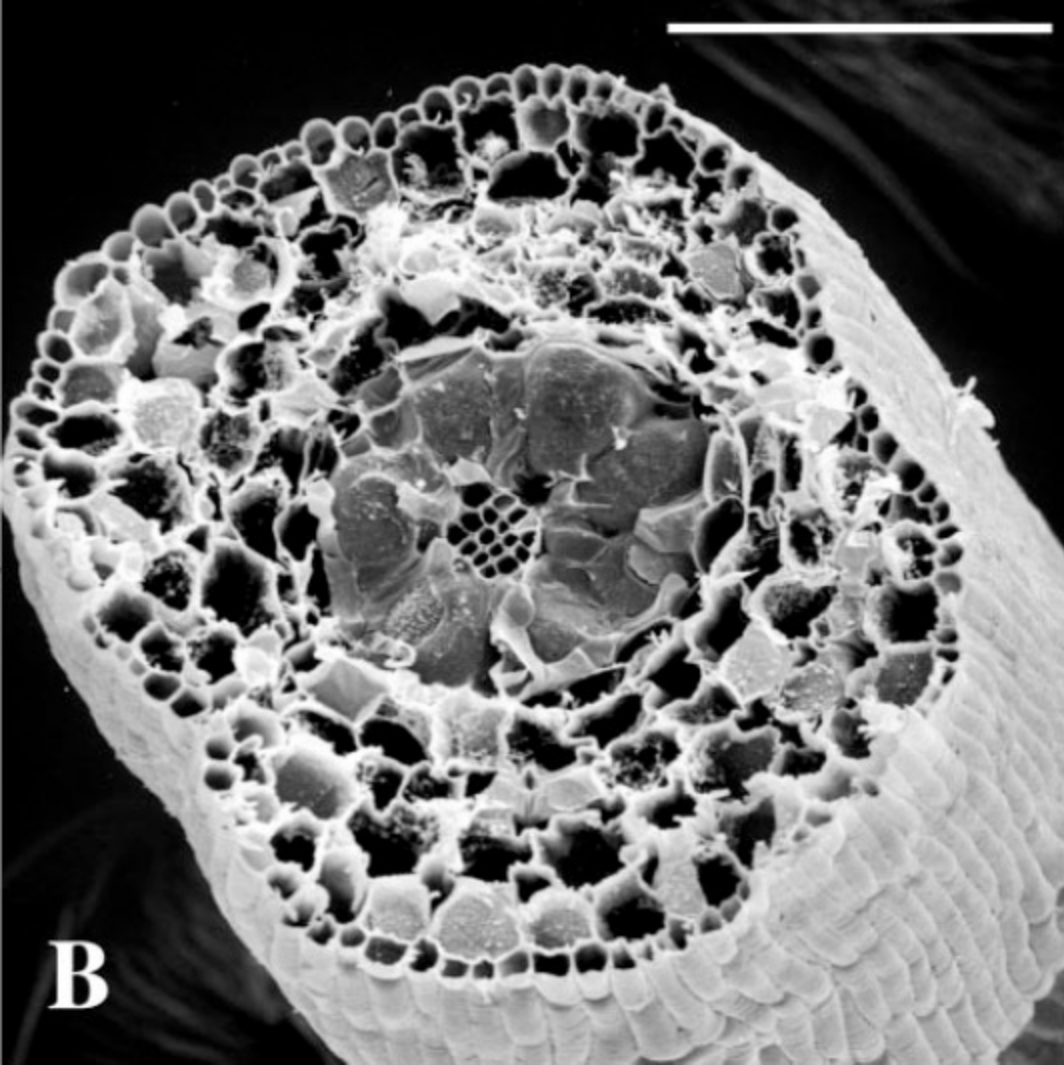
Dendroceros crispatus: группа
архегониев, в одном из них – молодой
спорогоний

Phaeoceros laevis,
3BC



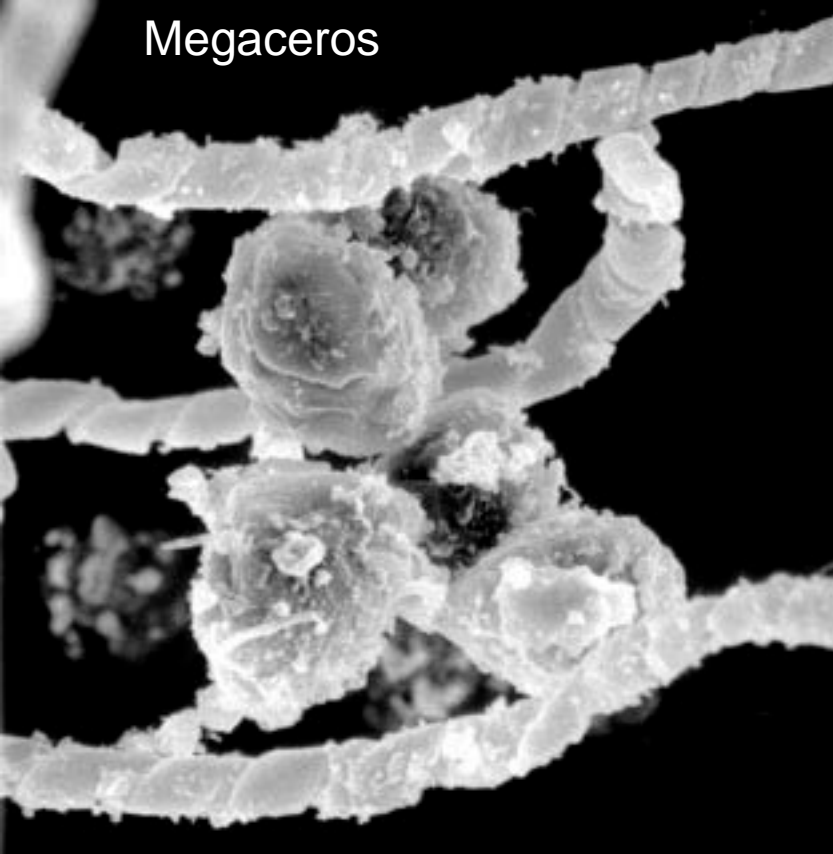


Phaeoceros,
ЗБС



Phaeoceros carolinianus

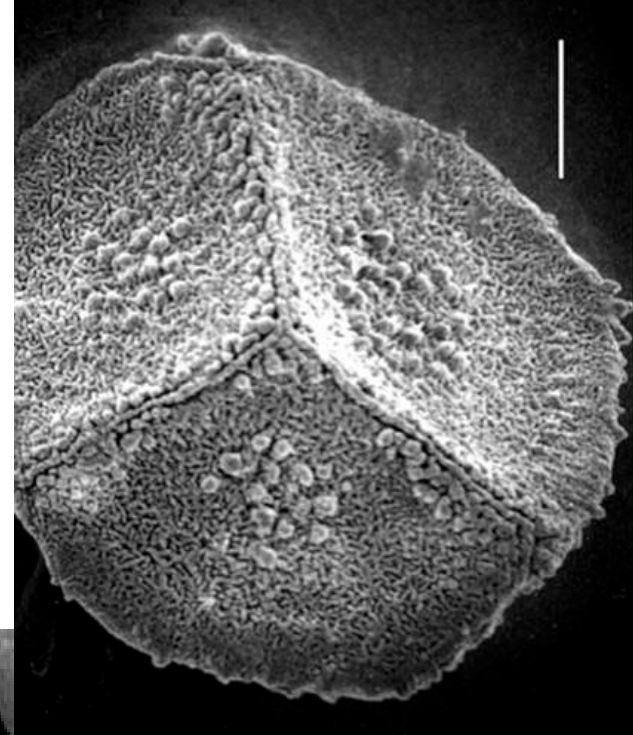
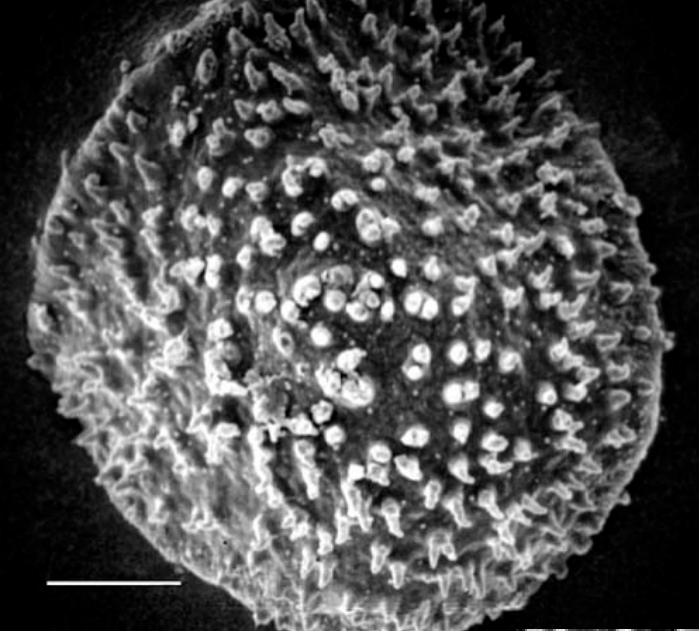
Megaceros



споры и
(псевдо)элатеры



*Phaeoceros
carolinianus*

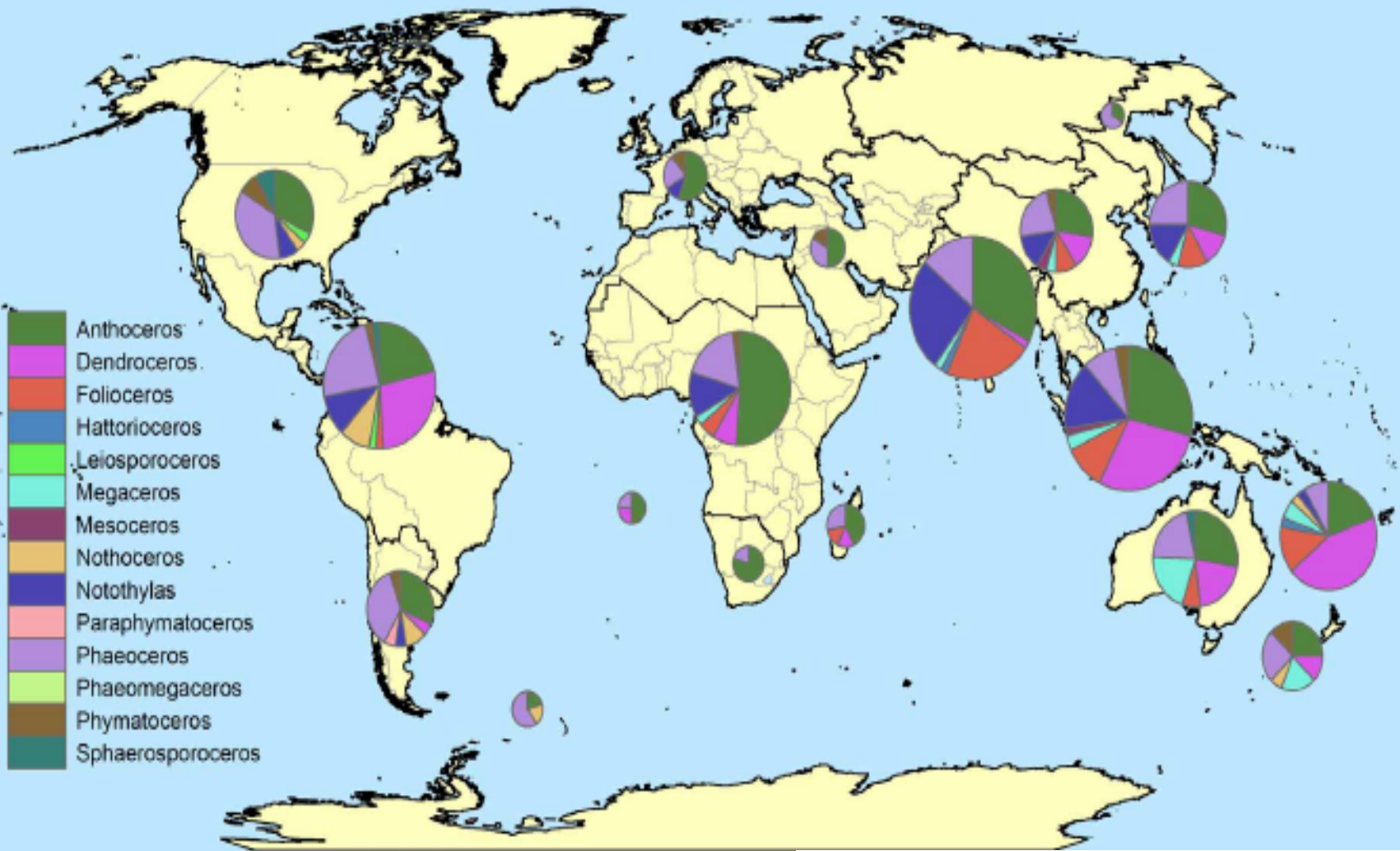


*спора с дистальной
стороны*

*спора с проксимальной
стороны*



тетрада спор



Всего: около 250 видов

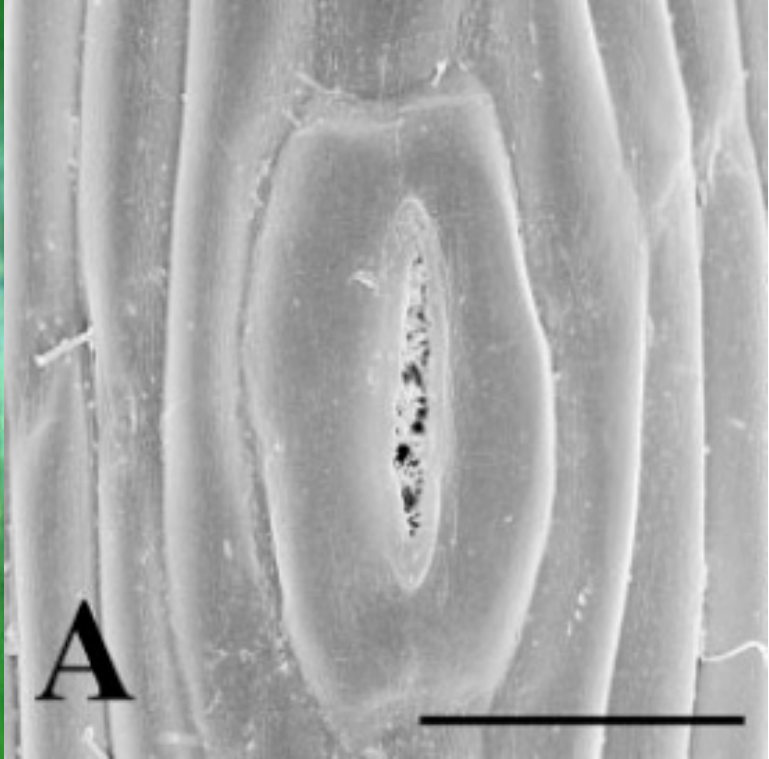
A synthesis of hornwort diversity: Patterns, causes and future work

JUAN CARLOS VILLARREAL¹, D. CHRISTINE CARGILL², ANDERS HAGBORG³, LARS SÖDERSTRÖM⁴ & KAREN SUE RENZAGLIA⁵

Proportion of hornwort species in the different genera across regions of the world. Size of the pie diagrams reflects the total number of species in that area (maximum 21 species).



Phaeoceros laevis



Phaeoceros carolinianus

устьице на стенке
коробочки

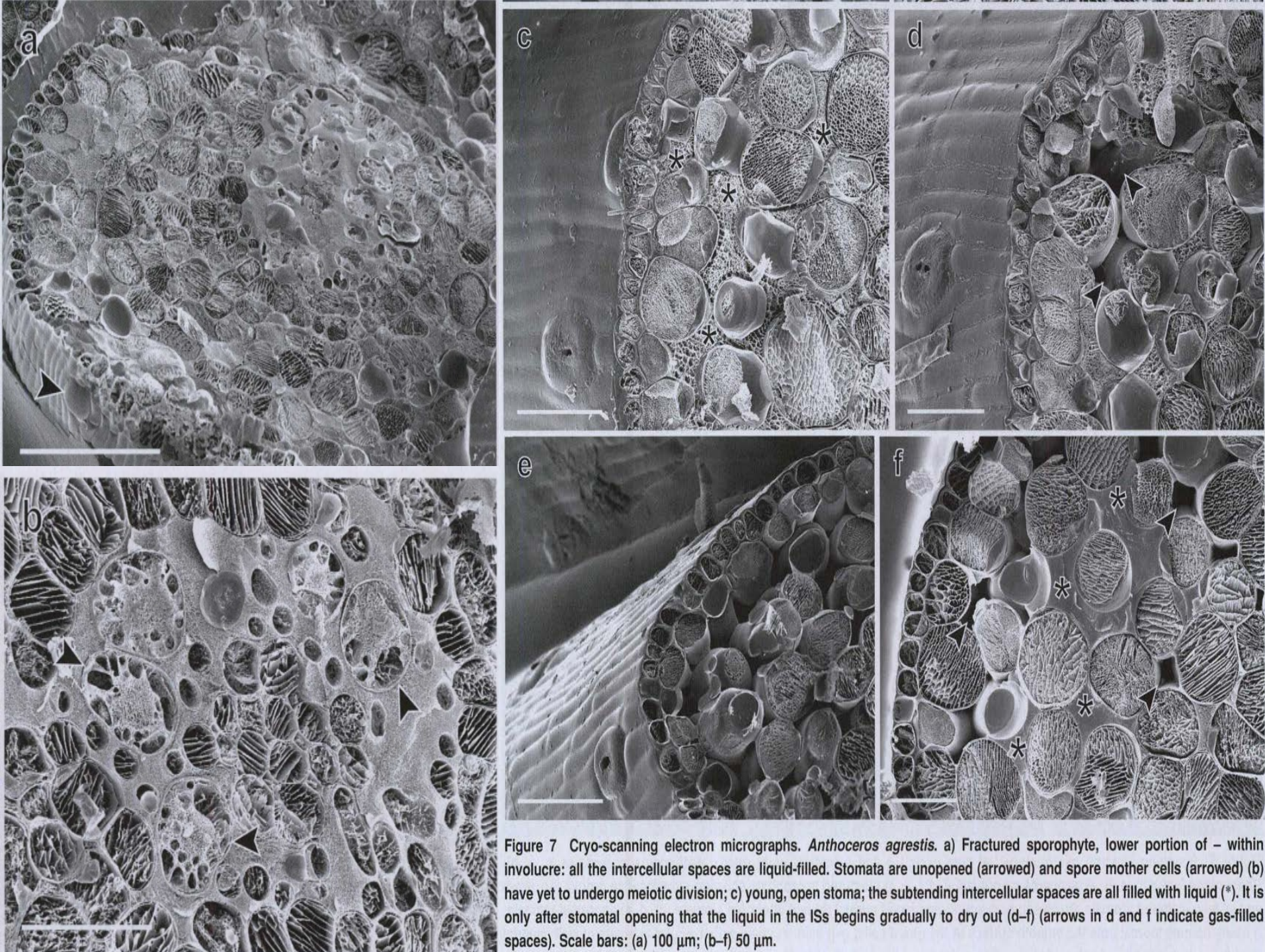
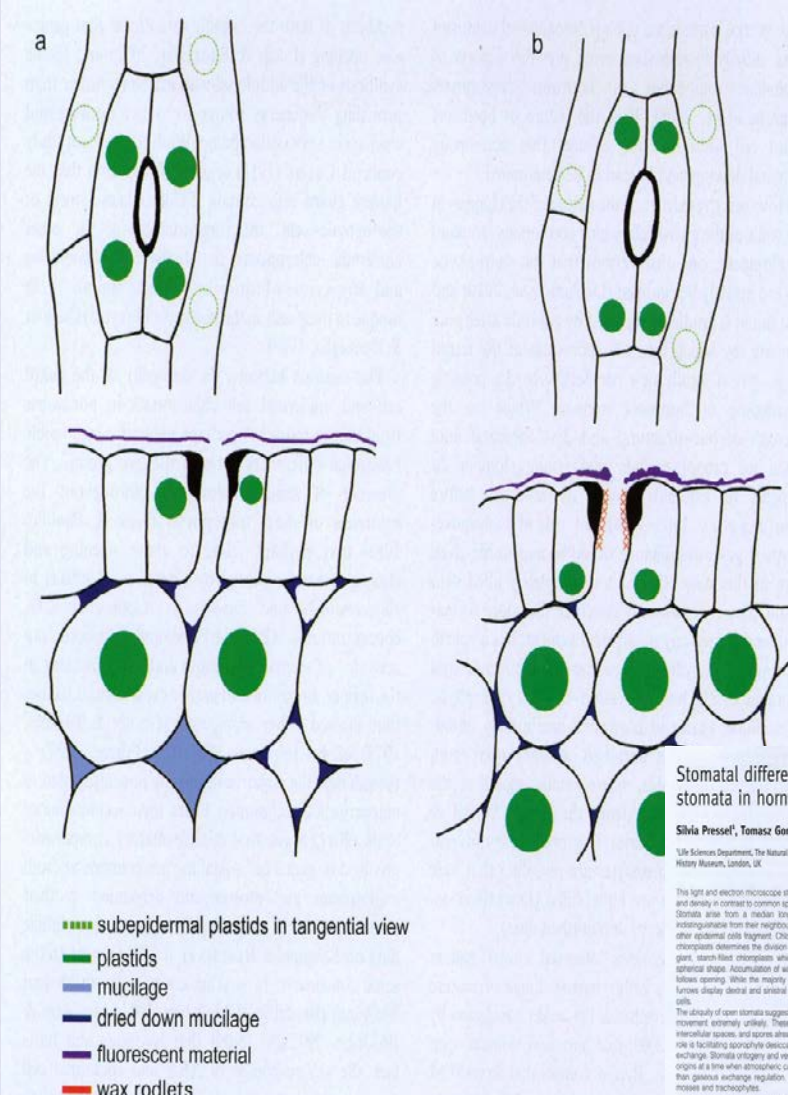
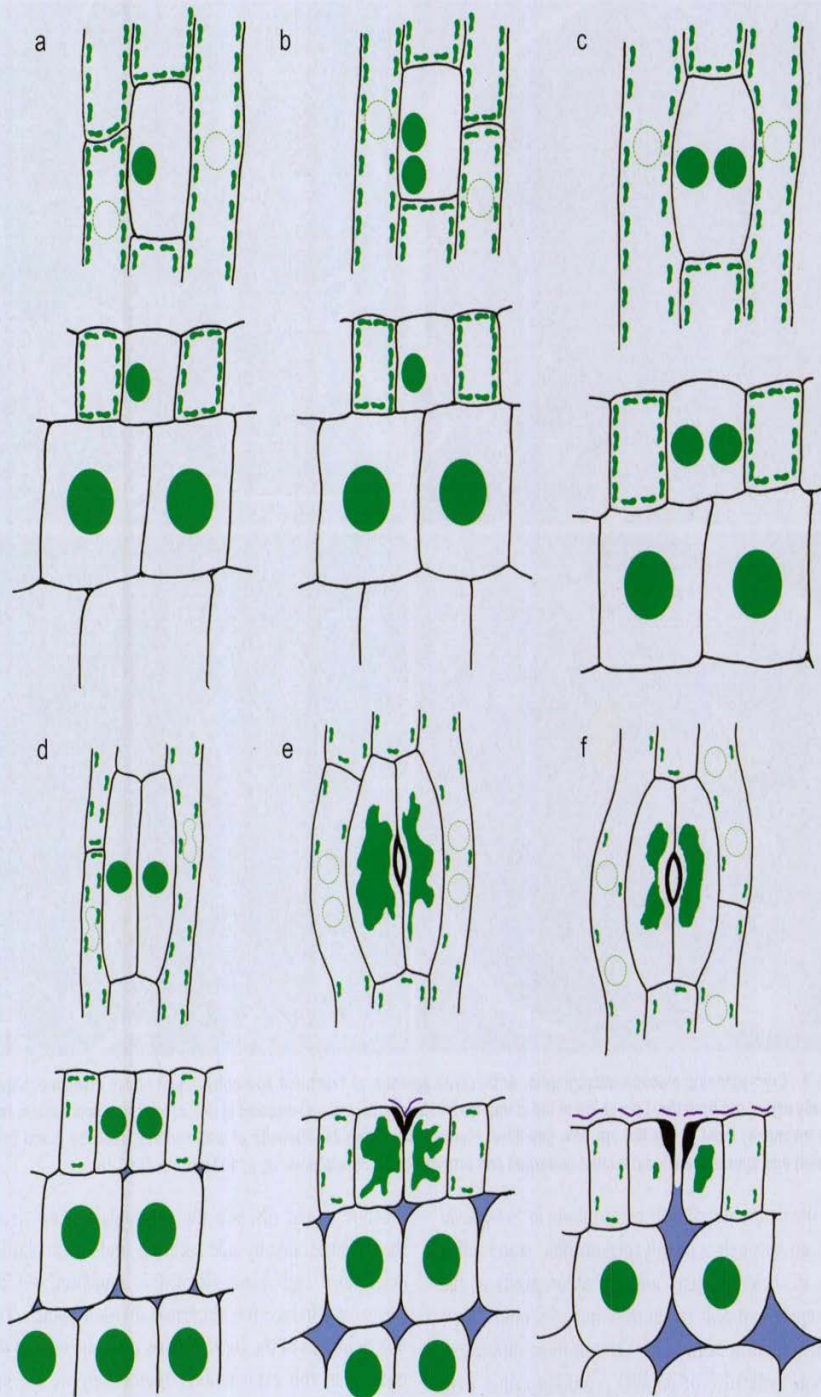


Figure 7 Cryo-scanning electron micrographs. *Anthoceros agrestis*. a) Fractured sporophyte, lower portion of – within involucre: all the intercellular spaces are liquid-filled. Stomata are unopened (arrowed) and spore mother cells (arrowed) (b) have yet to undergo meiotic division; c) young, open stoma; the subtending intercellular spaces are all filled with liquid (*). It is only after stomatal opening that the liquid in the ISs begins gradually to dry out (d–f) (arrows in d and f indicate gas-filled spaces). Scale bars: (a) 100 µm; (b–f) 50 µm.



■ subepidermal plastids in tangential view
■ plastids
■ mucilage
■ dried down mucilage
■ fluorescent material
■ wax rodlets

Figure 10 Schematic representation of stomatal ontogeny in hornworts; cont. from Fig. 9. a) Two spherical chloroplasts near the surface of each of the guard cells (Fig. 2g). The mucilage in the intercellular spaces below the epidermis has dried down to the cell corners but remains between the cells further inside the sporophytes (Fig. 7d, f); b) mature stoma with irregular deposits of fluorescent wall material covering the external surface (Figs. 5h, i; 6h, i); wax rodlets lining the pore (Fig. 6j) and chloroplasts lying along the inner walls of the guard cells (Fig. 2h–j). All the intercellular spaces are now gas-filled with dried-down mucilage along the cell junctions (Fig. 8a, c).

Figure 9 Schematic representation of stomatal ontogeny in hornworts; tangential views (top) and transverse sections (bottom). a) Nascent mother cells with a single spherical chloroplast (Fig. 1a); b) division of the mother cell chloroplast (Fig. 1 b–d); c) immediately before the longitudinal division of the mother cell the chloroplasts increase in size and migrate to lie side-by-side centrally (Fig. 1e); d) nascent stoma with each guard cell containing a single spherical chloroplast (Fig. 1f); the initial stage in aperture formation (Fig. 2a–c) coincides with division of the subepidermal chloroplasts and the almost complete disappearance of the fragmented epidermal cell chloroplasts. Huge pleiomorphic, starch-filled chloroplasts in the guard cells. Fluorescent additional wall material above the aperture (Fig. 5f, g). Mucilage-filled intercellular spaces (Fig. 7a, c); f) pore formation coinciding with division of the guard cell chloroplasts (Fig. 2d–f) and spread of fluorescent material over the external surface (Fig. 5h, i).

Stomatal differentiation and abnormal stomata in hornworts

Silvia Pressel¹, Tomasz Goral², Jeffrey G. Duckett¹

¹Life Sciences Department, The Natural History Museum, London, UK, ²Imaging and Analysis Centre, The Natural History Museum, London, UK

This light and electron microscope study reveals considerable uniformity in hornwort stomata morphology and density in contrast to common spatial and developmental abnormalities in tracheophytes and mosses. Stomata arise from a median longitudinal division of sporophyte epidermal cells morphologically indistinguishable from their neighbours apart from the selection of a single chloroplast which fuses in the other epidermal cells fragment. Chloroplast division and side-by-side repositioning of the two daughter chloroplasts determines the division plane in the stomatal mother cell. The nascent guard cells contain large, starch-filled sporopores which subsequently divide and, post aperture opening, regain their spherical shape. Accumulation of wall material over the guard cells and of wax rodlets lining the pores follows opening. While the majority of stomata are bilaterally symmetrical those lining the dehiscence furrows display dorsal and ventral asymmetry due to differential expansion of the adjacent epidermal cells. The ability of open stomata suggests that these never close with the multiaxial axis changes rendering movement extremely unlikely. These structural innovations: a liquid fluid stage in the ontogeny of the intercellular spaces, and apores already at the latest stage when stomata open, suggest that their primary role is facilitating sporophyte desiccation leading to dehiscence and spore dispersal rather than gaseous exchange. Stomata ontogeny and very low densities, like those in Devonian fossils, suggest other ancient origins at a time when atmospheric carbon dioxide levels were much greater than today or a function other than gaseous exchange regulation. We found no evidence for stomatal homology between hornworts, mosses and tracheophytes.

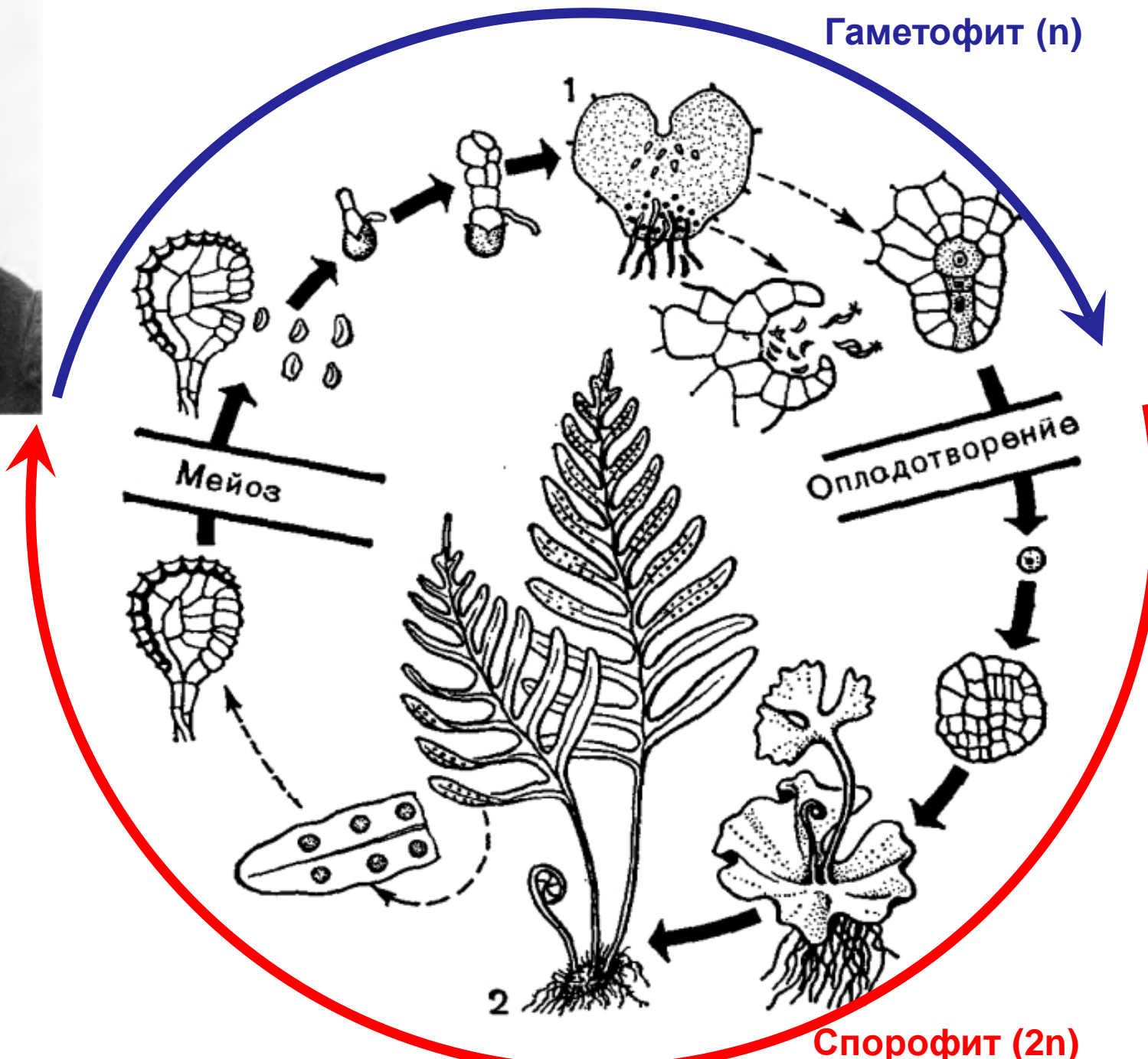
Introduction
 Genetic and hormonal manipulation of stomatal density in flowering plants (Zhu et al., 1976; Martin & Simons, 2001; Duboué-Lévesque et al., 2012; Zhang et al., 2012), together with investigations into the effects of carbon dioxide concentrations (McDermott & Chalmers, 1965; Woodward & Kelly, 1985; Beattie, 2002; Kattar et al., 2003), all at the forefront of current research on yield improvement and climate change. Although these experimental studies a wide variety of stomatal defects, affecting both guard cell and subsidiary cell morphology and number, have been reported from numerous vascular plants (Dodge, 1961; Takahashi, 1962; Isenhardt & Pridmore, 1989; Isenhardt et al., 1989; Cappel & Shah, 1970; Isenhardt et al., 1970; Isenhardt & Pridmore, 1976). In contrast, there has been very little thorough investigation of stomatal abnormalities in bryophytes. Kullback (1922) described several aberrant structures and suggested links between bryophyte stomata and those in protoleaves. Haberleitner (1986) and Paine & Paine (1957) reported the regular occurrence of stomata with 3 or 4 guard cells, which they regarded as 'false', in several groups of mosses. Paine and Paine (Paine, 1957; Paine & Paine, 1957) also recorded the occasional occurrence in mosses of two adjacent stomata at variance with the one cell opening rule (Kullack et al., 2005). In hornworts, Campbell (1955) described the stomata as arising from epidermal cells that cease to divide, become oval in shape and then divide longitudinally into one large guard cell whose median wall subsequently splits to form the pore. Whereas in many mosses the cells surrounding stomata can be distinguished from other epidermal cells by their radial arrangement (Paine, 1957), indicating that ontogeny depends on patterns of cell division extending beyond the guard cells, resulting in very similar situations in angiosperms (Ewers, 2006). In hornworts only a single epidermal cell is involved and the adjacent epidermal cells are unaffected.

Correspondence to: J. Pressel, Life Sciences Department, The Natural History Museum, Cromwell Road, London, UK. Email: j.p.1@nhm.ac.uk



Wilhelm Hofmeister (1824-1877)

профессор Гейдельбергского и Тюбингенского университетов, начал, идя по стопам отца, с того, что торговал музыкальными инструментами



Возможные родственные связи сосудистых растений



Сосудистые растения (Tracheophyta)

- преобладание спорофита в жизненном цикле
- обычно сложная гистологическая и морфологическая дифференциация спорофита, у современных форм обычно есть побеги и корни
- прочная кутикула; способность к синтезу суберина и лигнина (склереиды, волокна, *трахеальные элементы*).
- гаметофиты на теломном или талломном уровне организации
- архегонии погружены брюшком в ткань гаметофита (у продвинутых форм их нет)
- сперматозоиды исходно многожгутиковые (редко вторично 2-жгутиковые)
- за редкими исключениями, гомойогидрические растения

Возможные родственные связи сосудистых растений

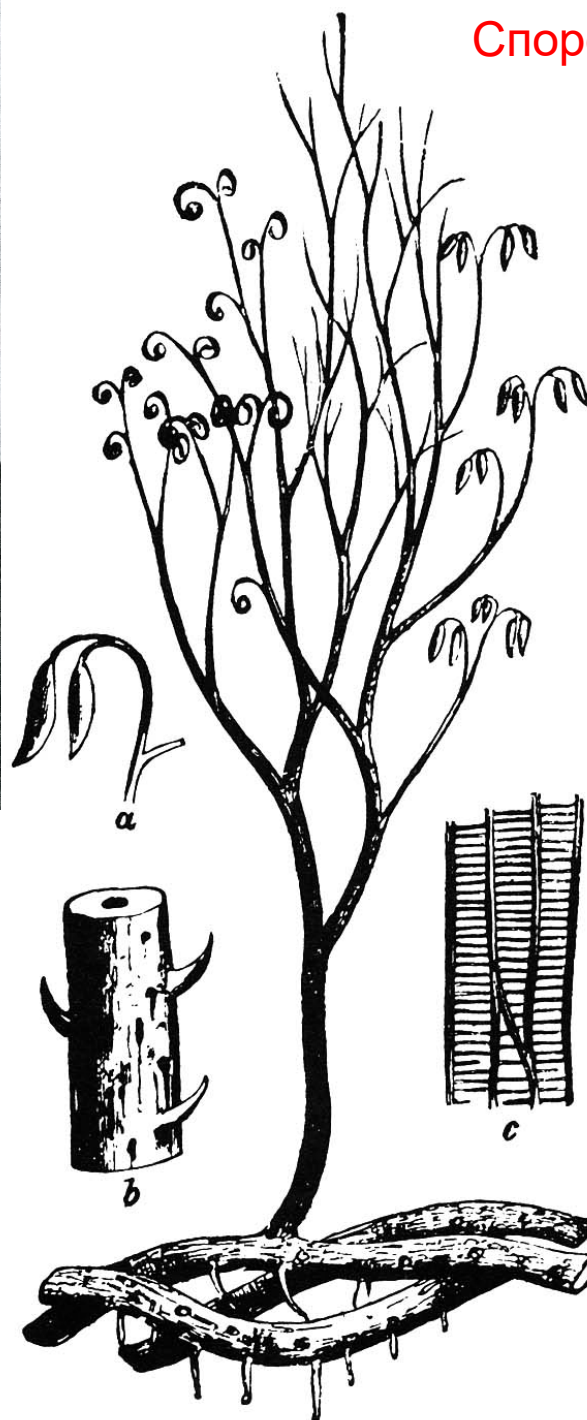


Сосудистые растения (Tracheophyta)

- преобладание спорофита в жизненном цикле
- обычно сложная гистологическая и морфологическая дифференциация спорофита, у современных форм обычно есть побеги и корни
- прочная кутикула; способность к синтезу суберина и лигнина (склереиды, волокна, *трахеальные элементы*).
- гаметофиты на теломном или талломном уровне организации
- архегонии погружены брюшком в ткань гаметофита (у продвинутых форм их нет)
- сперматозоиды исходно многожгутиковые (редко вторично 2-жгутиковые)
- за редкими исключениями, гомойогидрические растения



Спорофит!!!



Sir John William Dawson

(1820-1899)

1859 - впервые описал древнейшие ископаемые растения, в том числе

Psilophyton princeps

из отложений

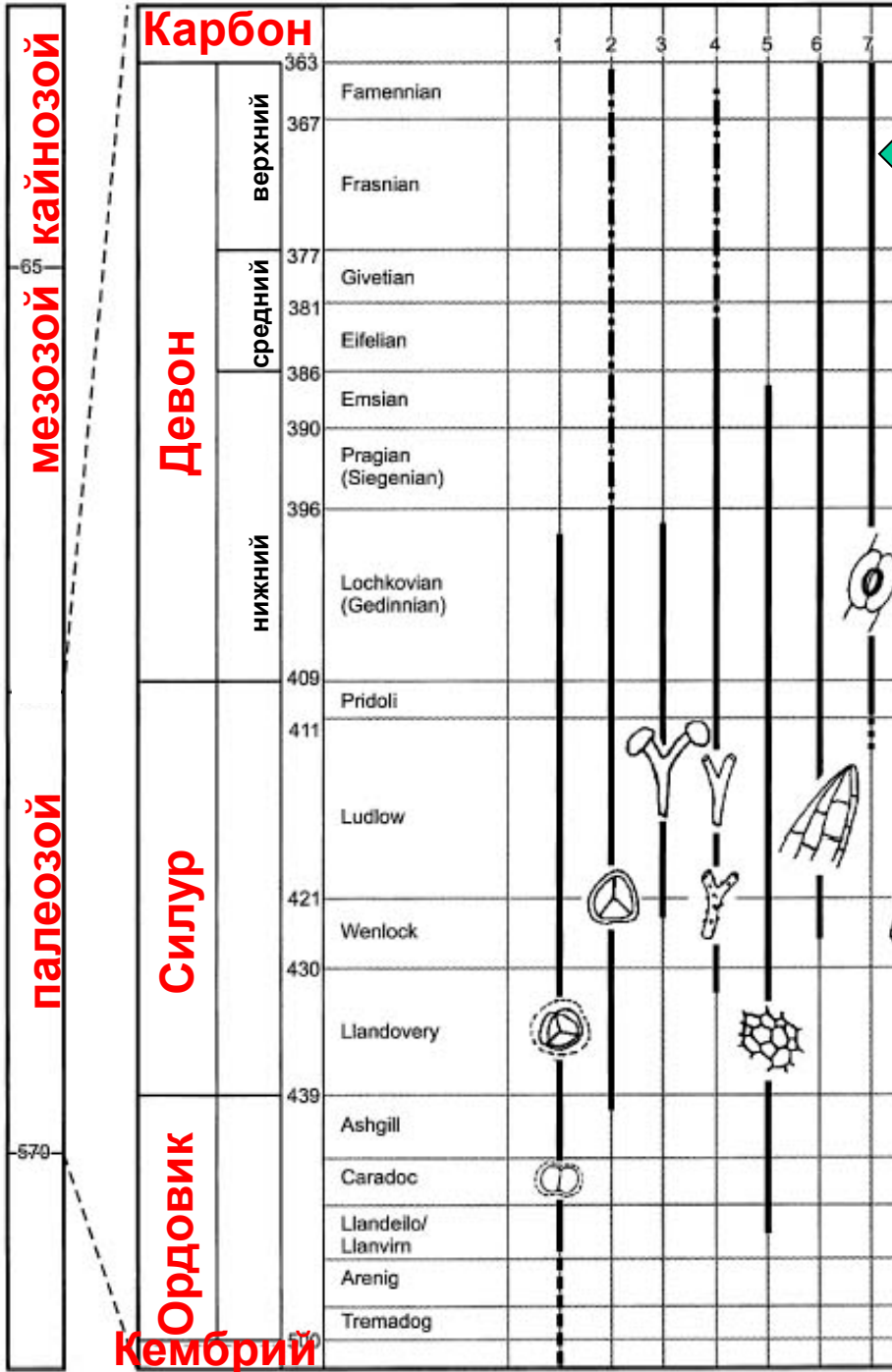
Gaspé Bay,

Quebec, Canada

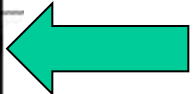
Был креационистом,
критиковал Дарвина с религиозных позиций

«правильный»
Psilophyton dawsonii

из Kenrick, Crane (1997)



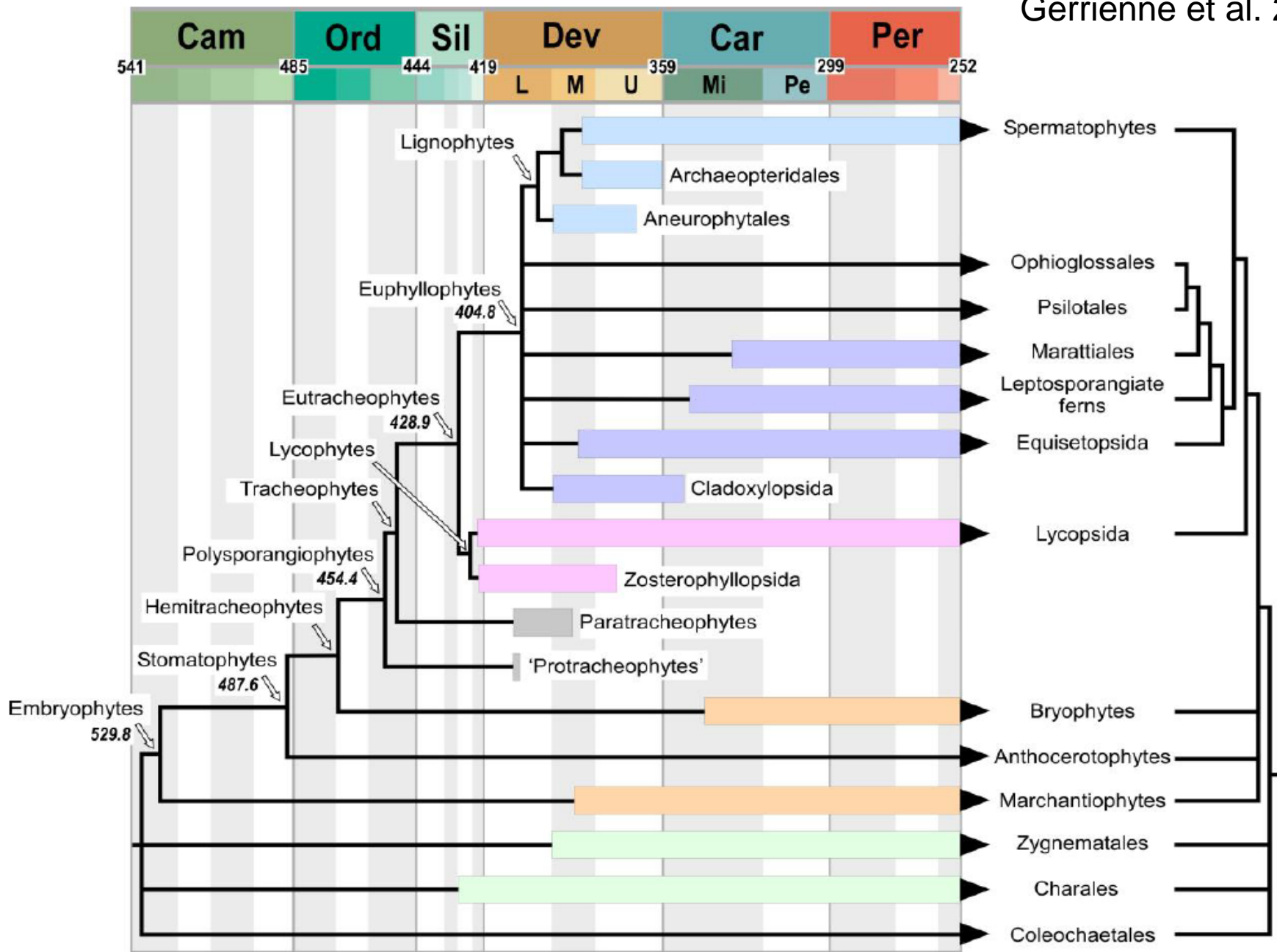
Традиционные представления о первых достоверных находках мохообразных.



Rhyne chert

(древнейшие сосудистые растения с полностью восстановленным жизненным циклом)





Морфология

ДНК

Oldest known mosses discovered in Mississippian (late Viséan) strata of Germany

Maren Hübers and Hans Kerp

Forschungsstelle für Paläobotanik, Institut für Geologie und Paläontologie, Westfälische Wilhelms-Universität Münster, Schlossplatz 9, 48143 Münster, Germany

ABSTRACT

The pre-Permian record of bryophytes is restricted to a very limited number of liverwort occurrences in Middle and Late Devonian and in Pennsylvanian strata, and a putative liverwort from the Middle Ordovician. The paucity of bryophytes, notably the apparent absence of mosses in the Carboniferous, is striking because this time interval is marked by the occurrence of extensive wetland environments that likely provided ideal habitats. We report three types of mosses from the Mississippian of eastern Germany that are the oldest unequivocal mosses known to date. Although the material is fragmentary, these finds show that mosses formed part of Carboniferous ecosystems. The moss remains were obtained by bulk maceration, a method that is not commonly used for studying Carboniferous floras. We anticipate that applying this method on material from other Carboniferous localities will show that mosses were more widespread in the late Paleozoic than previously thought.

GEOLOGICAL SETTING, AGE, AND METHODS

The mosses described here were collected from a roadcut of the A4 motorway near Chemnitz-Glösa, Saxony, Germany (50°52'34.67"N; 12°54'38.73"E), where an 80-m-thick succession of Mississippian sandstones, shales, and occasional coaly layers of the upper part of the Ortelsdorf Formation (Hainichen Subgroup, Hainichen Basin) is exposed (Schneider et al., 2005). The small Hainichen Basin (Fig. 1) is filled with alluvial plain, alluvial fan, and fan

Несомненные сосудистые растения известны из силура и массово встречаются в девоне.

Лишь очень немногочисленные печеночники известны из девона, а мхи вообще достоверно не обнаружены древнее карбона.

GEOLOGY, August 2012; v. 40; no. 8; p. 755–758;

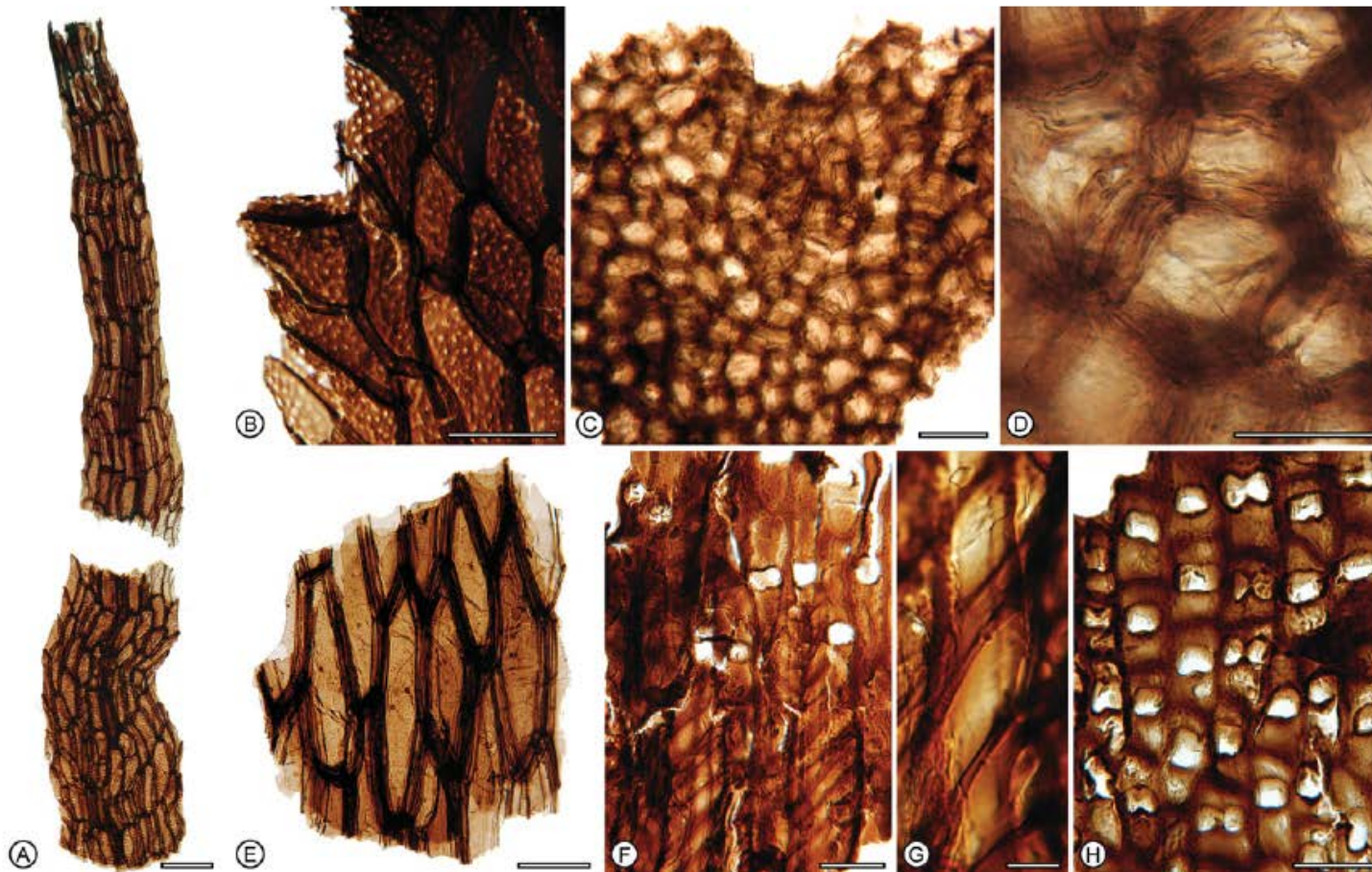
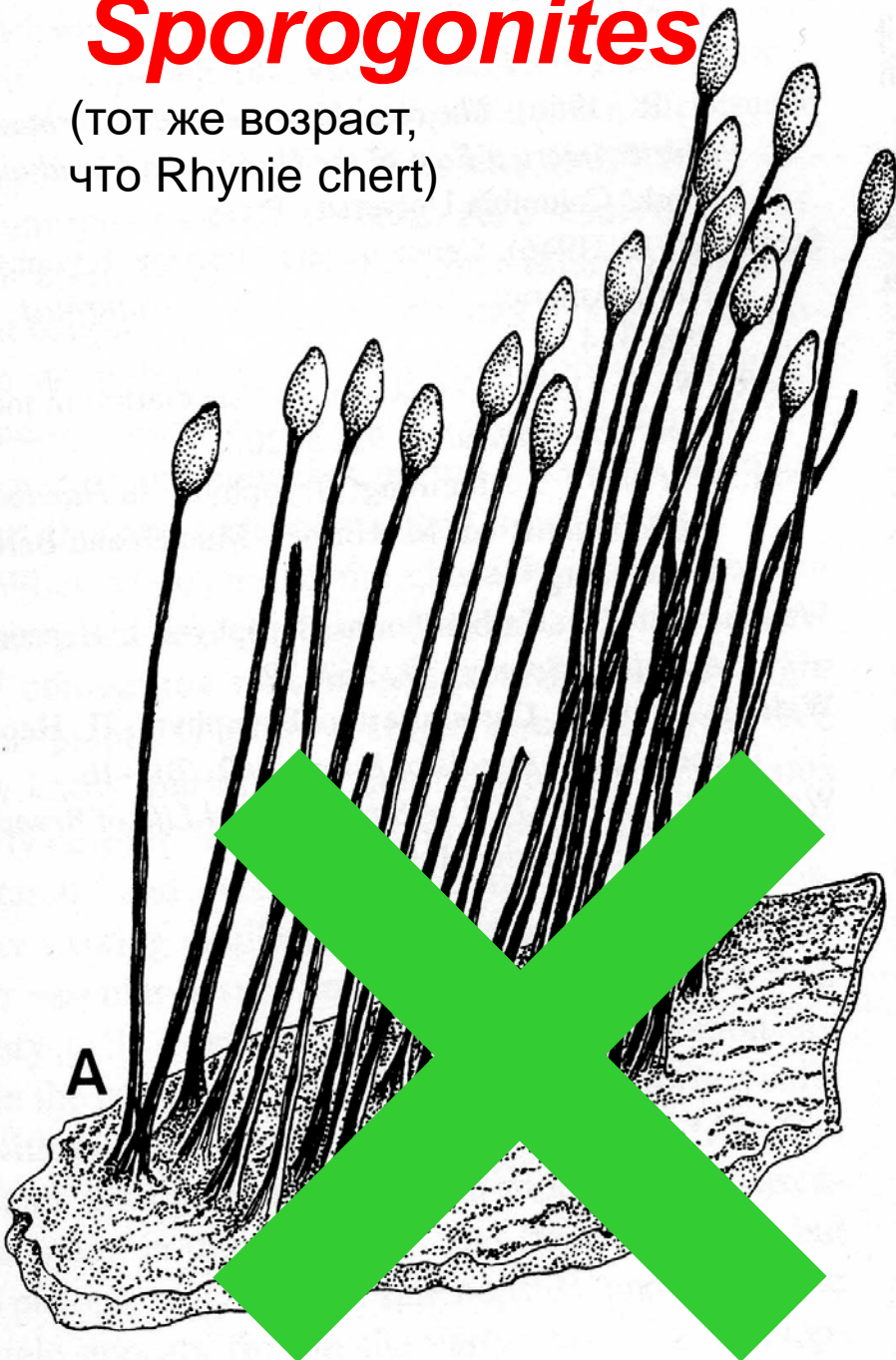


Figure 3. Mosses from Viséan of Glösa. A: Type I. Almost complete leaf (KS27–074); scale bar = 100 μ m. B: Type I fragment (KS27–031); scale bar = 50 μ m. C: Type II. Overview showing network formed by darker cells and fenestrae with lighter colored cells (KSgrPr-068); scale bar = 100 μ m. D: Detail of C showing elongate cells forming network; scale bar = 50 μ m. E: Type II. Bistratose fragment with more elongate cells (KS11–090); scale bar = 100 μ m. F: Type III. Elongate cells with pores and fibrils (KS11–029); scale bar = 30 μ m. G: Type III. Detail of F (fibrils), scale bar = 10 μ m. H: Type III. Another form with short cells with pores (KS27–048); scale bar = 50 μ m.

Sporogonites

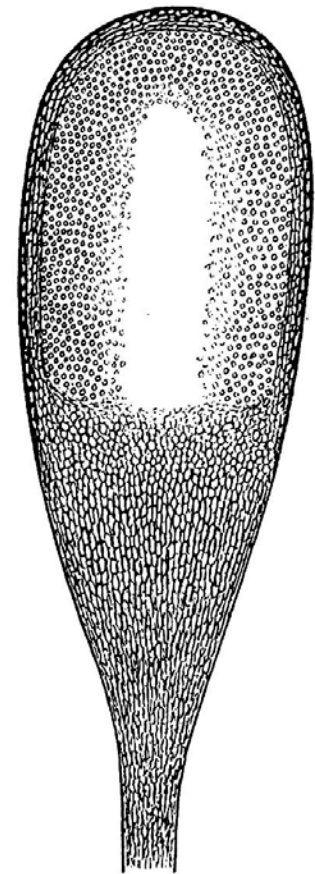
(тот же возраст,
что Rhynie chert)



a

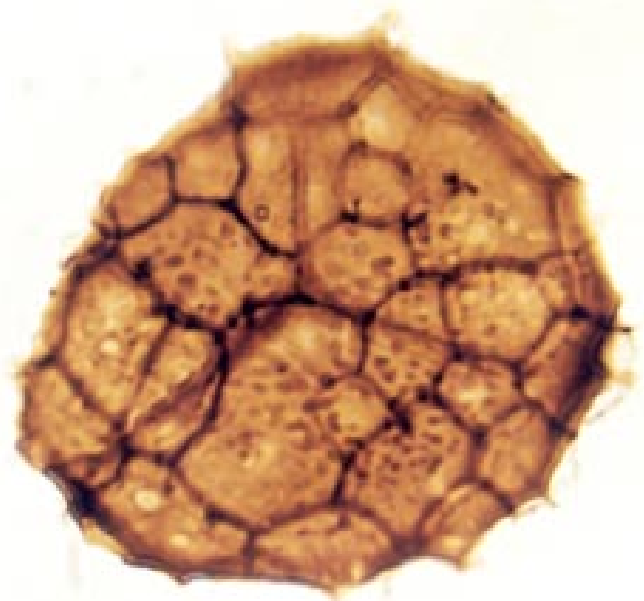


b



c

FIGURE 4.18. *Sporogonites exuberans*. Drawings reproduced from Halle 1936a (Figure 1), with permission. (a) Sporangium (capsule) fragment showing five short vertical slits (dehiscence features?) on the outer surface ($\times 2$). (b) Sporangium terminal on slender axis ($\times 2$). (c) Partial reconstruction of sporangium showing parts of interior and exterior ($\times 7$). Spore sac surrounds a central sterile region (columella?).



споры древнейших
известных
ископаемых высших
растений

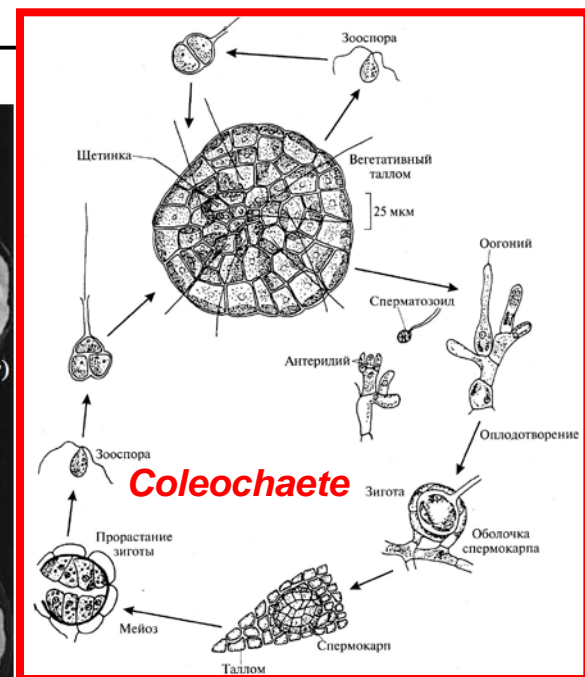
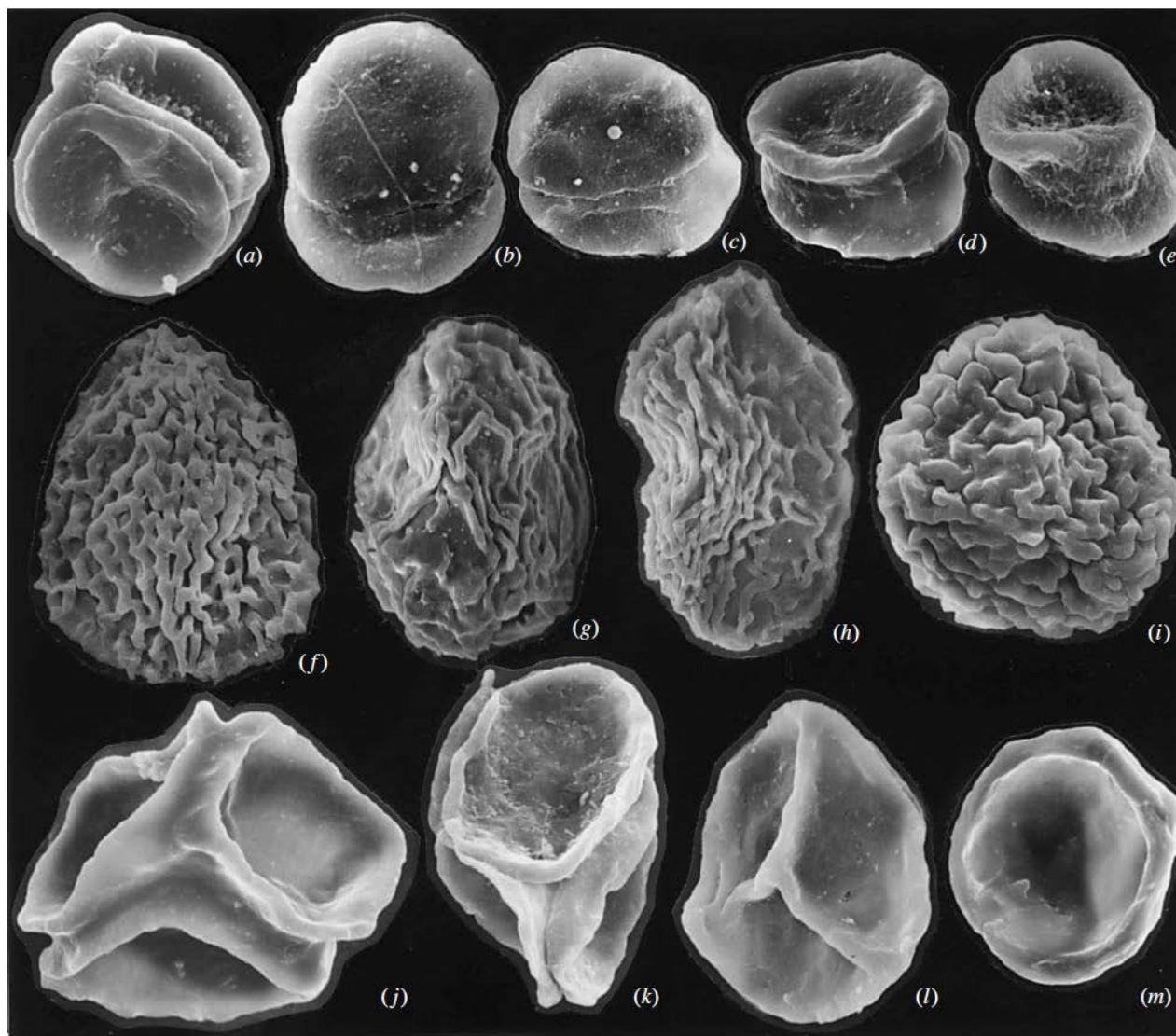


Figure 3. SEM images of dispersed early land plant spores. (a–i) From the type area for the Caradoc, Shropshire, England (Caradoc, Late Ordovician) (Wellman 1996); (j–m) from the Silurian inliers along the southern margin of the Midland Valley of Scotland (early Wenlock, Late Silurian) (Wellman & Richardson 1993). (a) Naked, unfused, permanent tetrad ($\times 2000$); (b,c) naked, unfused, permanent dyad ($\times 1500$); (d,e) naked, fused, permanent dyad ($\times 1500$); (f–h) envelope-enclosed permanent dyad ($\times 1500$); (i) envelope-enclosed permanent tetrad ($\times 1500$); (j) naked, permanent tetrad ($\times 1210$); (k) loose tetrad ($\times 1070$); (l) laevigate trilete spore ($\times 1380$); (m) laevigate hilate monad ($\times 1230$).

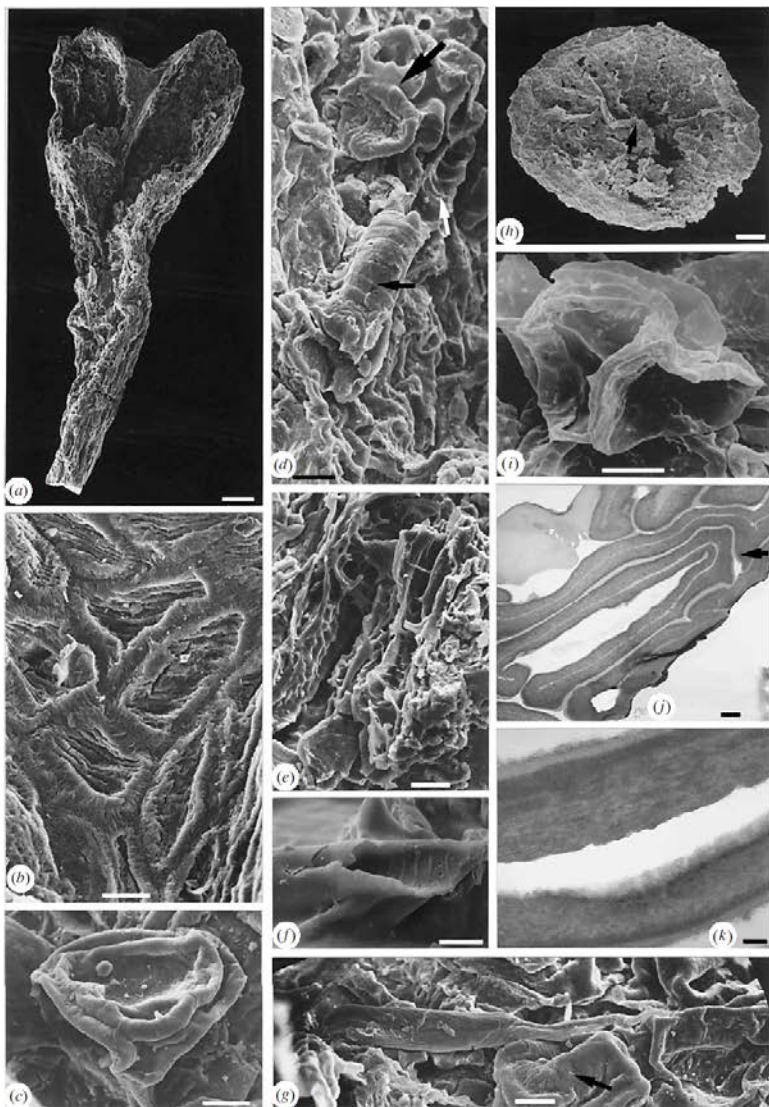


Figure 2. (a–k) North Brown Clec Hill specimens, Shropshire, Lochkovian, Lower Devonian. (a–e, g) SEMs: *Grisellatheca salopensis*, NMW94.76G.1. (a) Entire specimen with bifurcating terminal region. Scale bar = 100 μ m. (b) Surface at bifurcation. Scale bar = 10 μ m. (c) *In situ* tetrad with laevigate surface; ?*Cheilotetras*. Scale bar = 10 μ m. (d) 'Banded' tube in fertile region (small arrows) and remains of spore tetrad (large arrow). Scale bar = 10 μ m. (e) Longitudinal elements with irregular thickenings from centre of axis. Scale bar = 10 μ m. (g) Possible clater. Arrow indicates spore tetrad. Scale bar = 10 μ m. (f) 'Banded' tube attached by amorphous material to surface of a *Tortilicaulis* sporangium. NMW96.5G.9. Scale bar = 10 μ m. (h–k) ?Cuticle enclosed flattened spore mass. NMW98.23G.3. (h) SEM: intact specimen. Arrow indicates possible attachment site. Scale bar = 100 μ m. (i) SEM: isolated tetrad. Scale bar = 5 μ m. (j, k) TEMs. (j) Part of a tetrad. Arrow indicates possible apertural fold. Note sections through sporangial covering (top left) are of same optical density as outer layer surrounding each spore. Scale bar = 500 nm. (k) Trilayered exospore. Lightest layer to outside. Scale bar = 100 nm.

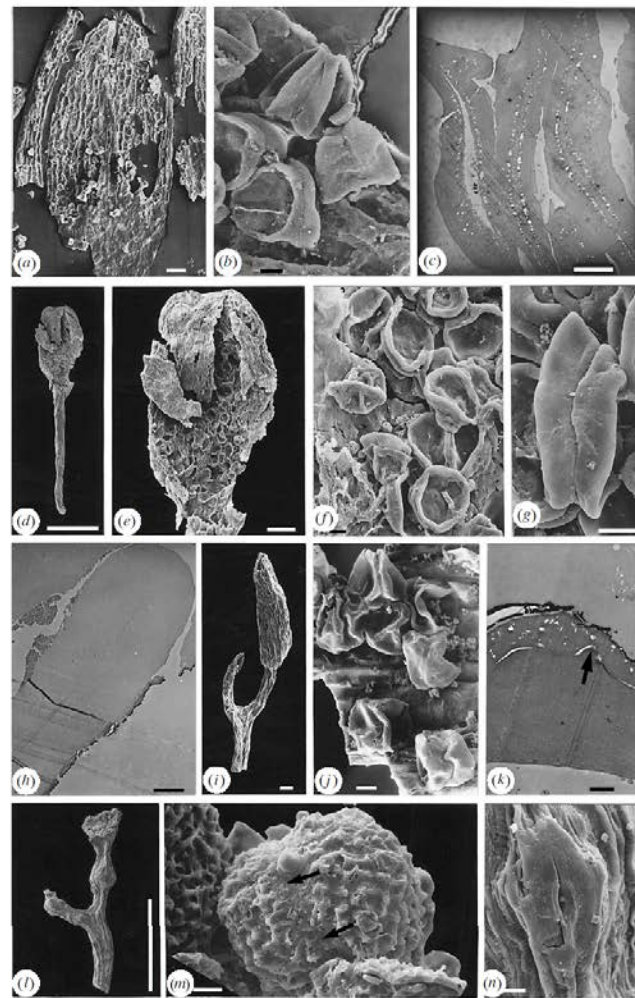


Figure 4. *In situ* permanent dyads. All North Brown Clec Hill, Shropshire, Lochkovian, Lower Devonian. (a–c) Sporangial cuticle with adhering laevigate dyads. NMW97.42G.1. (a) SEM: central cuticle probably representing one complete valve. Scale bar = 100 μ m. (b) SEM: cluster of probably naked dyads with deeply invaginated distal surfaces. Scale bar = 10 μ m. (c) TEM: walls of several spores. Note row of voids close to lumen in otherwise homogeneous exospore. Scale bar = 250 nm. (d–h) *Cullulitheca richardsonii*, NMW96.11G.6. (d) SEM: entire specimen. Scale bar = 500 μ m. (e) SEM: sporangium enlarged. Scale bar = 100 μ m. (f) SEM: *in situ* laevigate dyads with distal invaginations. Scale bar = 10 μ m. (g) SEM: single dyad showing contact feature. Scale bar = 10 μ m. (h) TEM: homogeneous exospore with some attached extra-exosporeal material. Scale bar = 1 μ m. (i, j) SEMs: *Fusitheca fanningiae*, NMW97.42G.4. (i) Intact specimen. Scale bar = 100 μ m. (j) Laevigate dyads attached to inside of sporangial wall. Scale bar = 10 μ m. (k–n) Naked bifurcating axis with vestiges of a terminal sporangium. NMW99.19G.1 (courtesy of K. Habgood). (k) TEM: homogeneous exospore and envelope with voids. Arrow indicates ornament on spore. Dark line is gold coating. Scale bar = 500 nm. (l) SEM: intact specimen. Swelling on axis is probably a taphonomic artefact. Scale bar = 1 mm. (m) SEM: single tetrad with envelope. Arrows indicate position of contact between spores. Scale bar = 10 μ m. (n) SEM: stoma. Scale bar = 10 μ m.

**Permanent spore dyads are not ‘a thing of the past’: on their occurrence in the liverwort
Haplomitrium (Haplomitriopsida)**

KAREN S. RENZAGLIA^{1*}, BARBARA CRANDALL-STOTLER¹, SILVIA PRE¹,
JEFFREY G. DUCKETT², SCOTT SCHUETTE³ and PAUL K. STROTHER⁴

Botanical Journal of the Linnean Society, 2015,

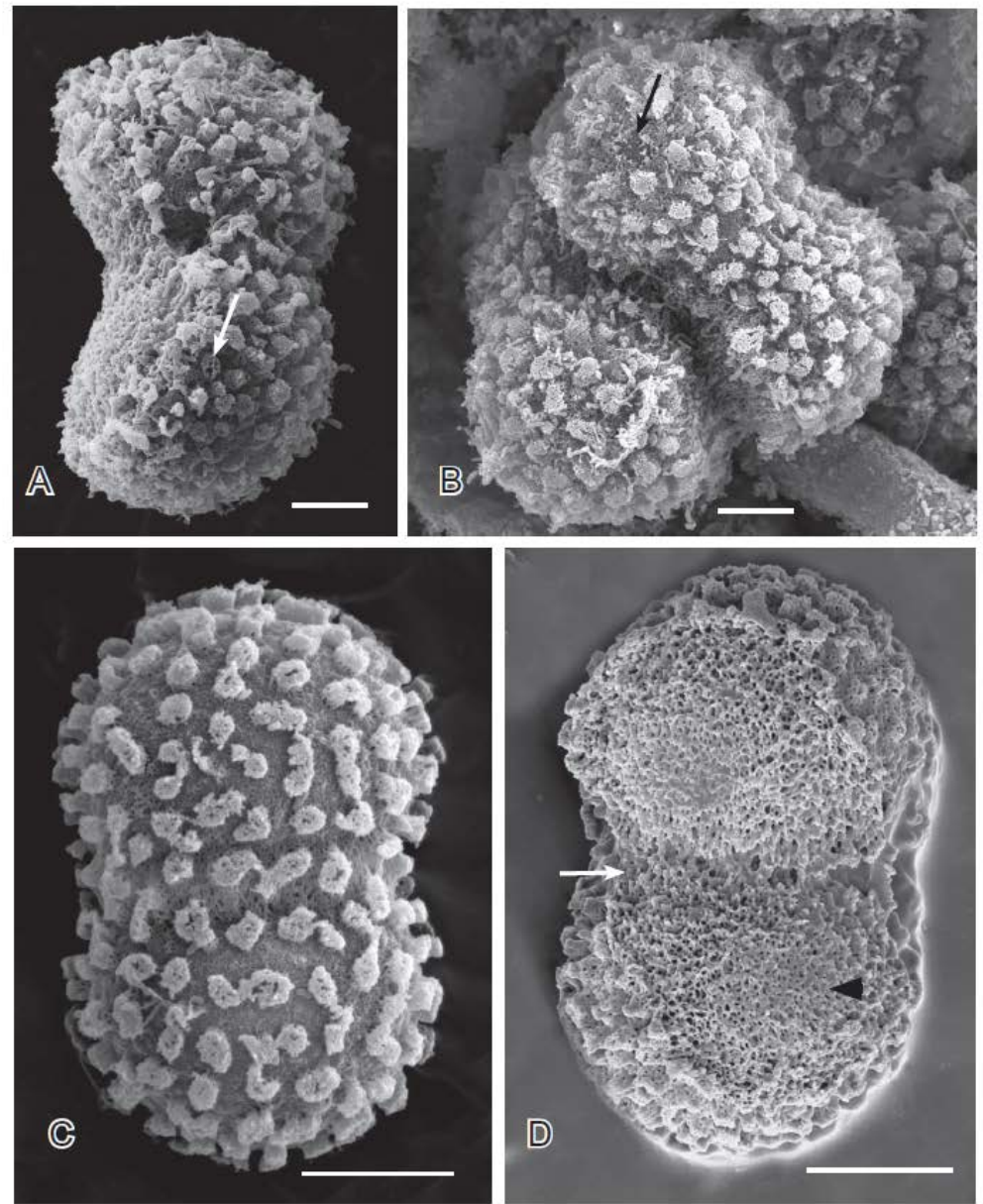


Figure 2. Scanning electron micrographs of dyads and a tetrad of the two populations of *Haplomitrium gibbsiae*. A, Chilean dyad in side view showing flattened proximal and rounded distal surfaces. Tubercles with caps decorate the distal surface with small holes on the wall between. Arrow indicates cap that detached during specimen preparation. B, Chilean tetrad showing dyad arrangement. Arrow indicates entire tubercle that detached during specimen preparation. C, Distal surface of New Zealand dyad showing tubercles that are continuous across spore boundaries. D, Flattened proximal surface of New Zealand dyad with reticulate sculptoderm and small irregular upright rods. Arrow indicates exine elements connecting the two spores and arrowhead points to dense central reticulum of exine elements. Bars, 10 μ m.

Семейство Cooksoniaceae

Это семейство мы не можем отнести ни к
одному из трех отделов современных
сосудистых растений

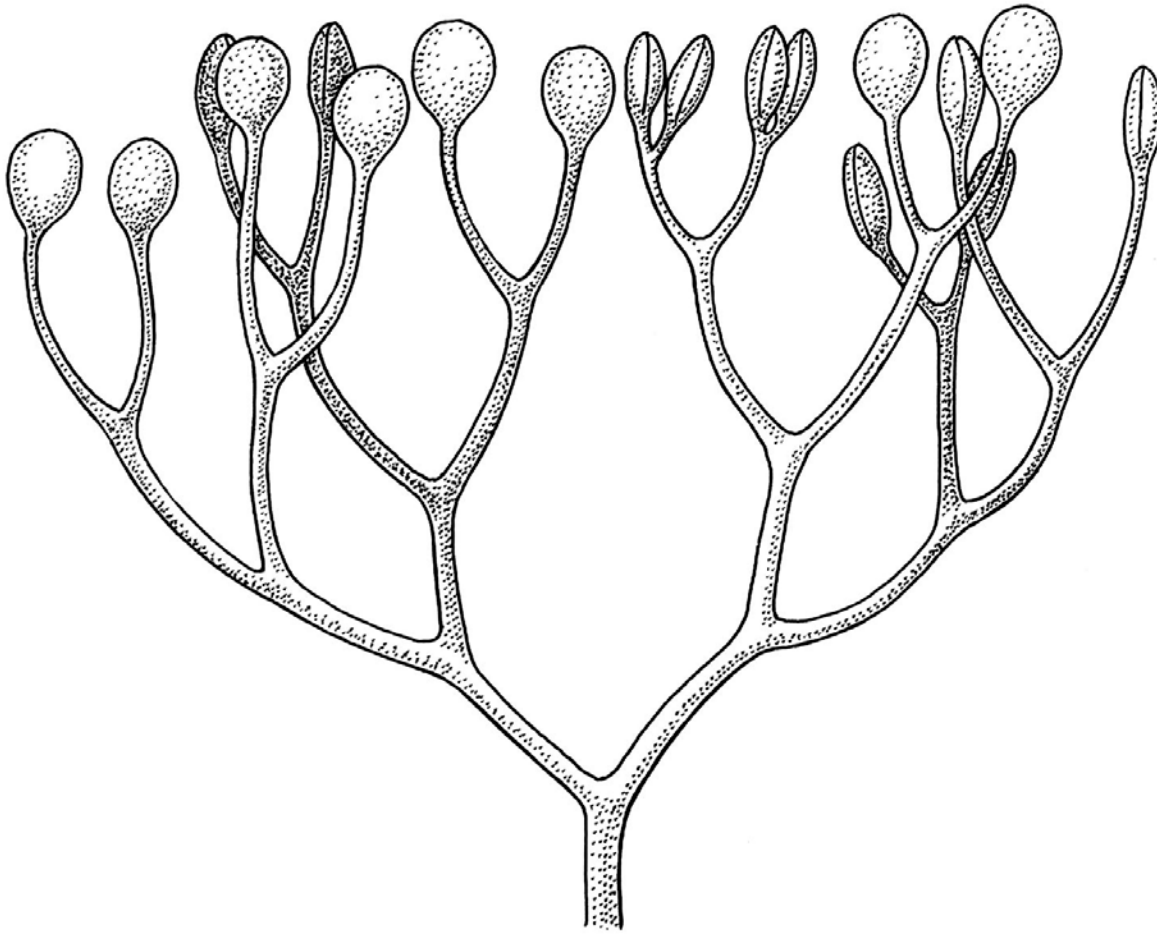
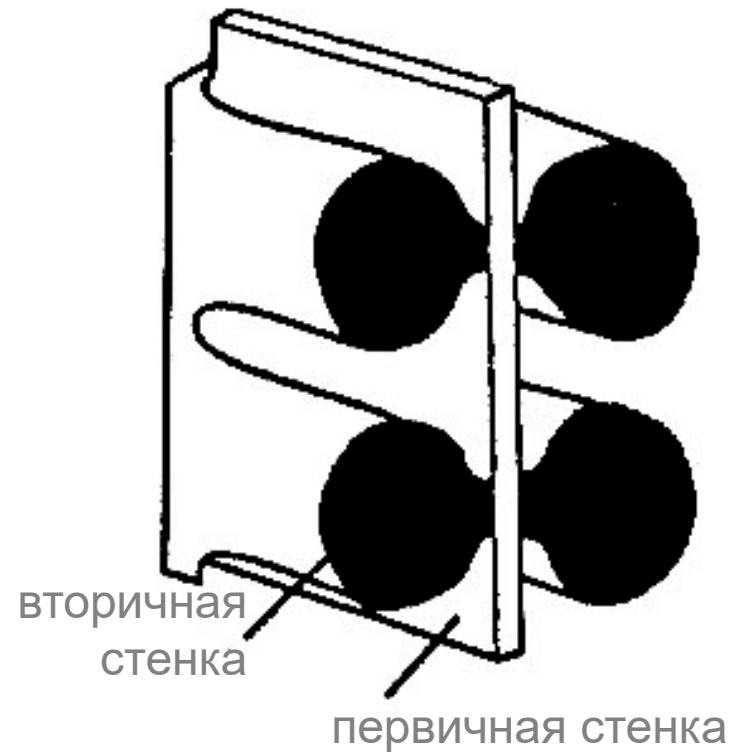
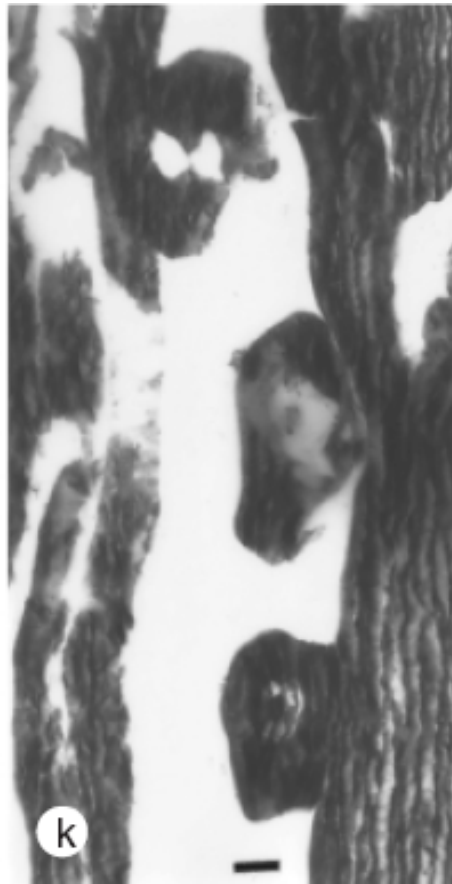


FIGURE 4.10. Reconstruction of distal parts of *Uskiella spargens* showing terminal spatulate sporangia with distal isovalvate dehiscence on isotomous branching axes ($\times 1$). Redrawn from Shute and Edwards 1989, Figure 71.

Семейство *Cooksoniaceae*

тонкое строение стенок трахеид



Тонкое строение трахеид – примерно как у современных сосудистых растений, но больше толщина первичной клеточной стенки

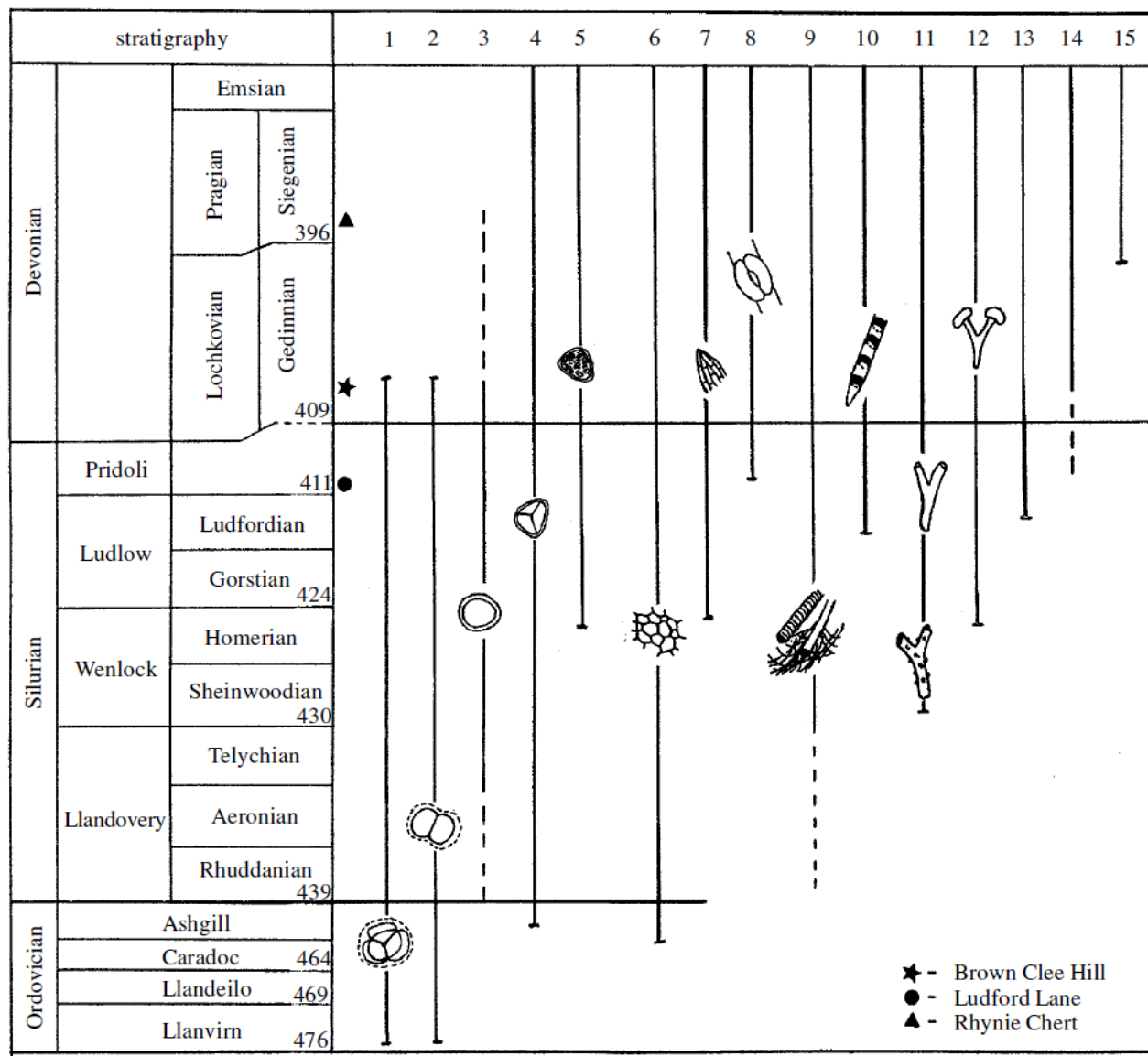


Figure 1. Stratigraphic ranges of fossils mentioned in text. 1, permanent (obligate) tetrads \pm envelope; 2, permanent dyads \pm envelope; 3, hilate monads; 4, trilete laevigate monads; 5, ornamented trilete monads; 6, cuticular sheets (cf. *Nematothallus*); 7, sporangial cuticles; 8, stomata; 9, associations of tubes, solid line only indicates presence of banded tubes; 10, tracheids; 11, bifurcating axes of ?tracheophyte type; 12, *Cooksonia*/Rhyniopsida; 13, Lycopytina sensu lato; 14, zosterophylls; 15, Trimerophytina.



[http://www.uni-muenster.de/GeoPalaeontologie/
Palaeo/Palbot/erhynie.html](http://www.uni-muenster.de/GeoPalaeontologie/Palaeo/Palbot/erhynie.html)
<http://www.abdn.ac.uk/rhynie/intro.htm>

Rhynie

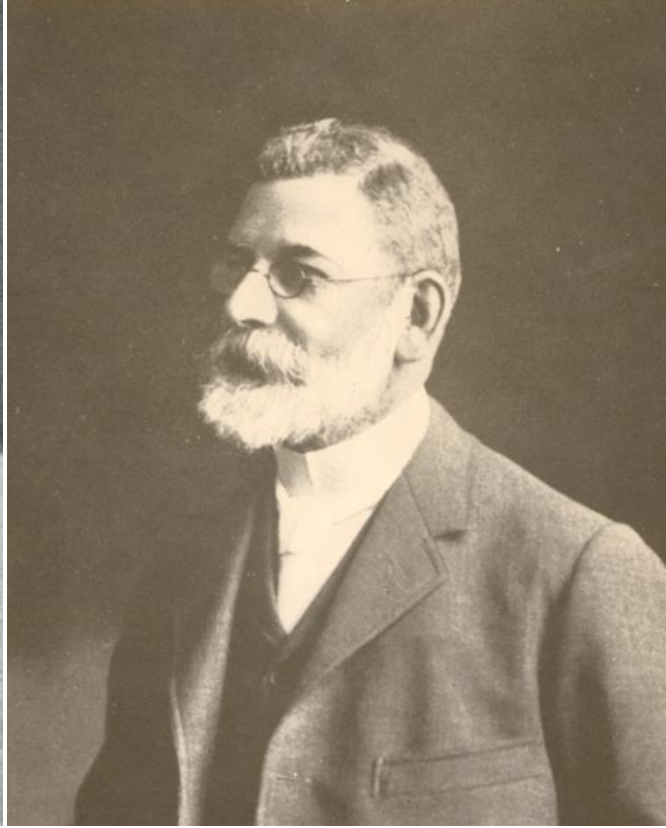
Rhynie chert (400 млн лет)



Современный аналог: Yellowstone National Park



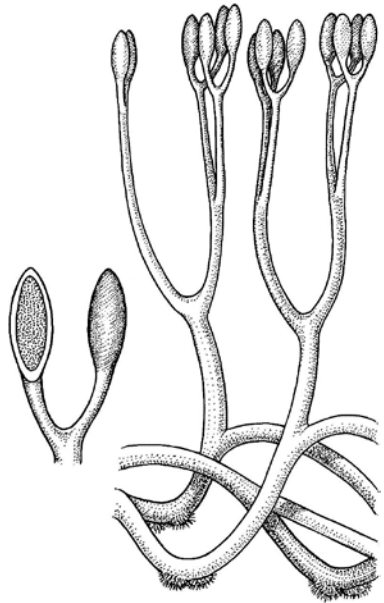
The Rhynie chert was discovered in 1912 by **Dr William Mackie**, a medical practitioner from the town of Elgin to the north of Rhynie



Dr Robert Kidston
Вместе с Henry Lang первыми научно описали ископаемые в 1917

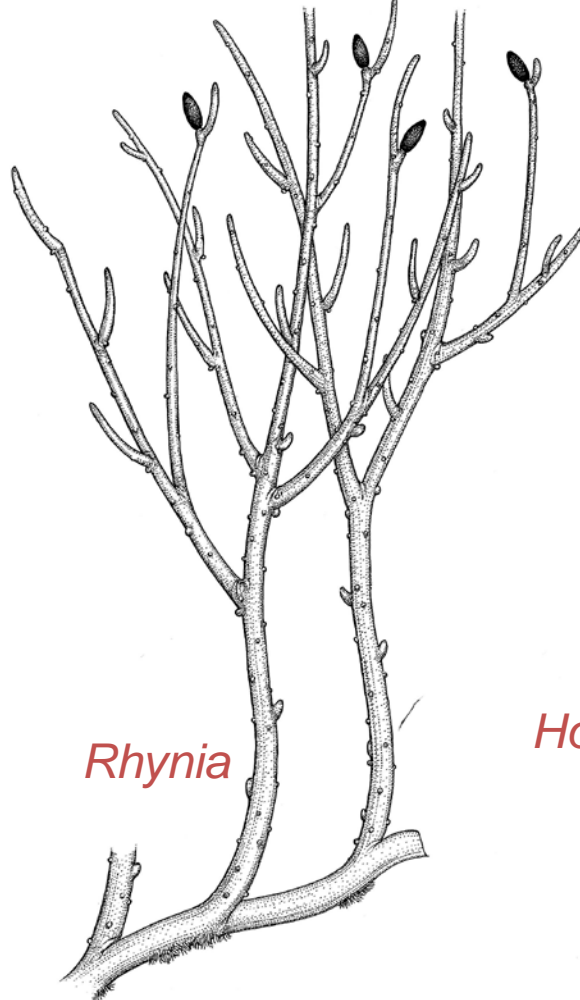


Dr Geoffrey Lyon возродил интерес к материалу из Rhynie в 1950 г. и описал прорастание спор, положив начало пониманию жизненного цикла ископаемых



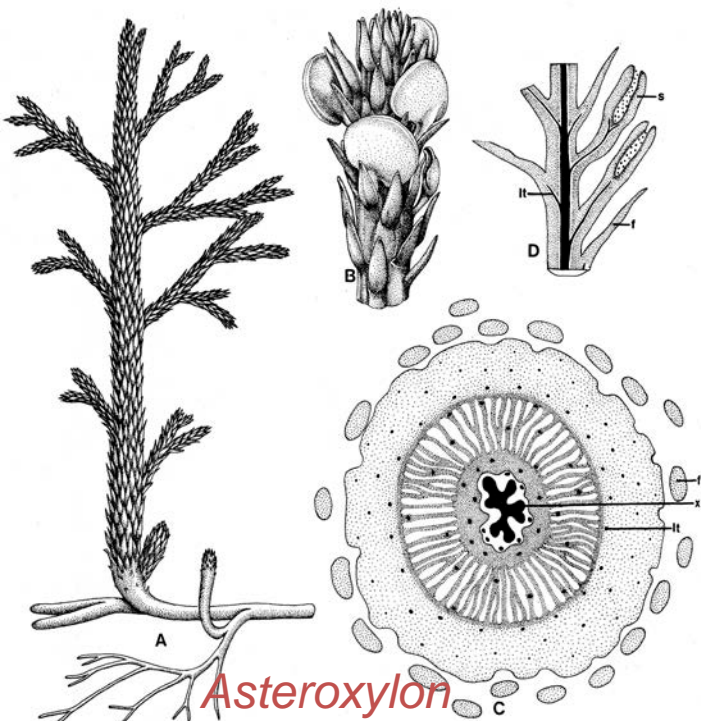
Aglaophyton

Nothia



Rhynia

Horneophyton



Asteroxylon

Это только *некоторые* из растений, найденных в Rhynie chert.

Некоторые (не изображенные здесь) растения из Райни описаны только в последние годы!

Все найденные здесь высшие растения – сосудистые. Мохообразных нет!

Aglaophyton major

высота – не более 30 см

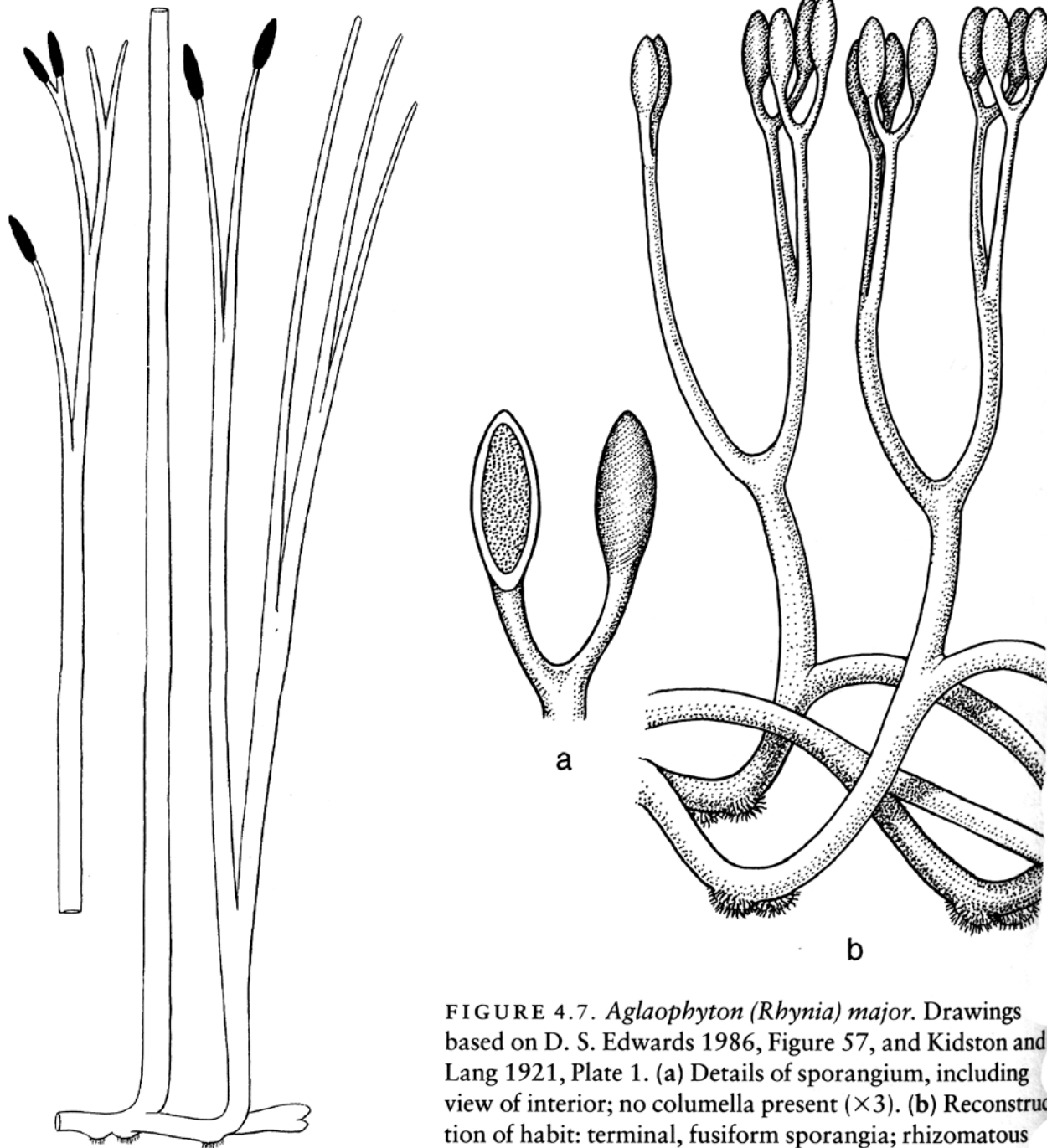
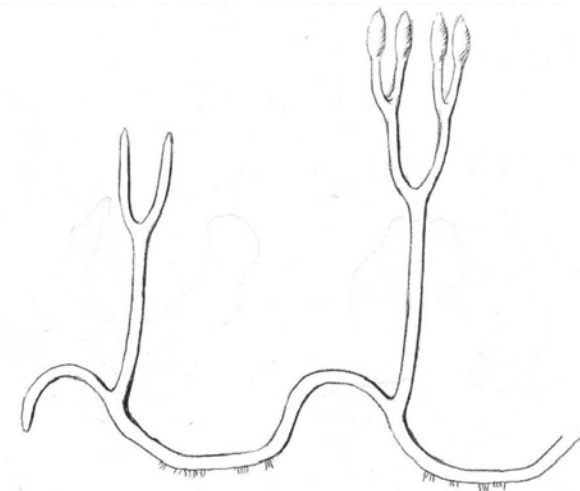
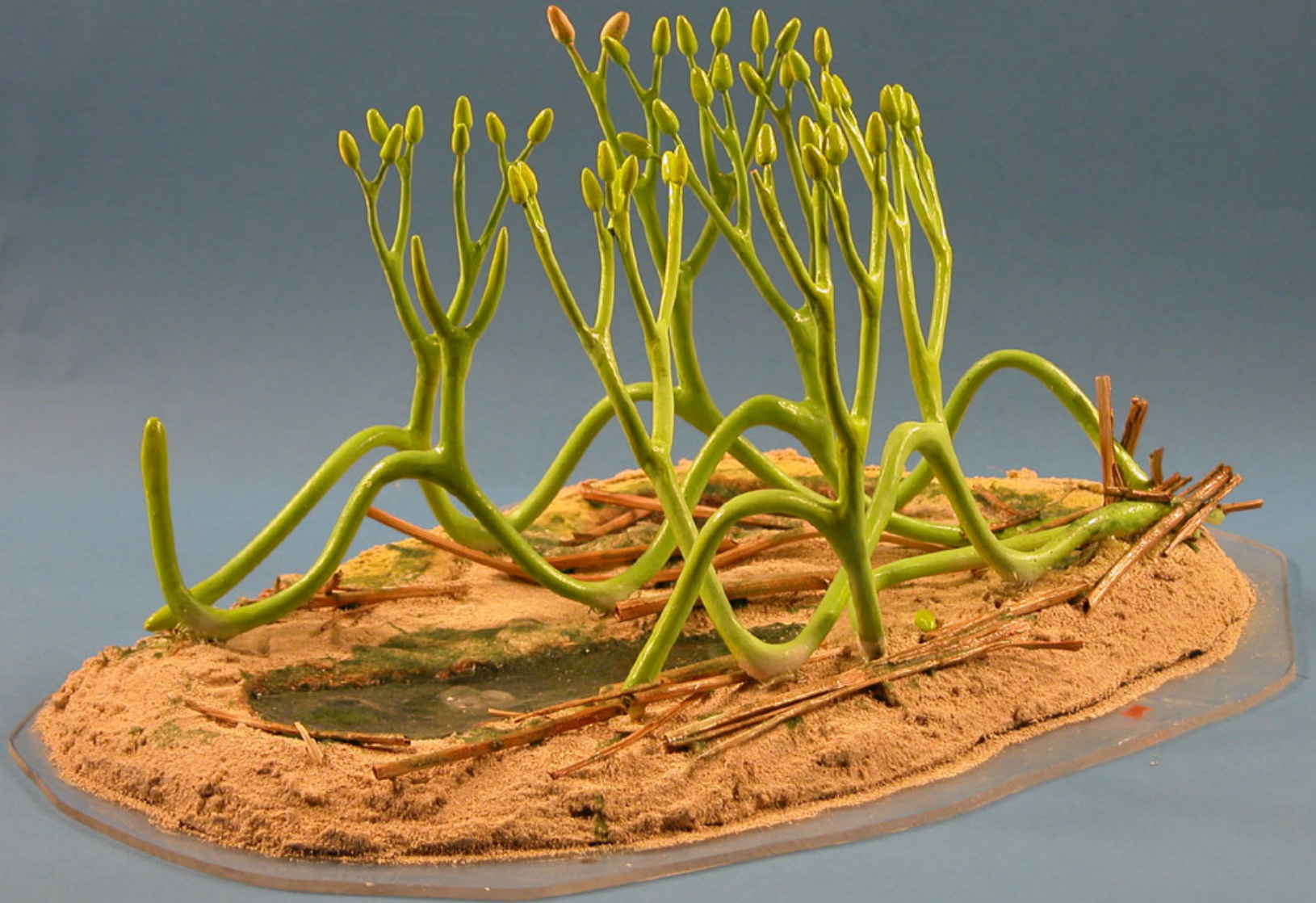


FIGURE 4.7. *Aglaophyton (Rhynia) major*. Drawings based on D. S. Edwards 1986, Figure 57, and Kidston and Lang 1921, Plate 1. (a) Details of sporangium, including view of interior; no columella present ($\times 3$). (b) Reconstruction of habit: terminal, fusiform sporangia; rhizomatous axes with clusters of unicellular rhizoids ($\times 0.8$).

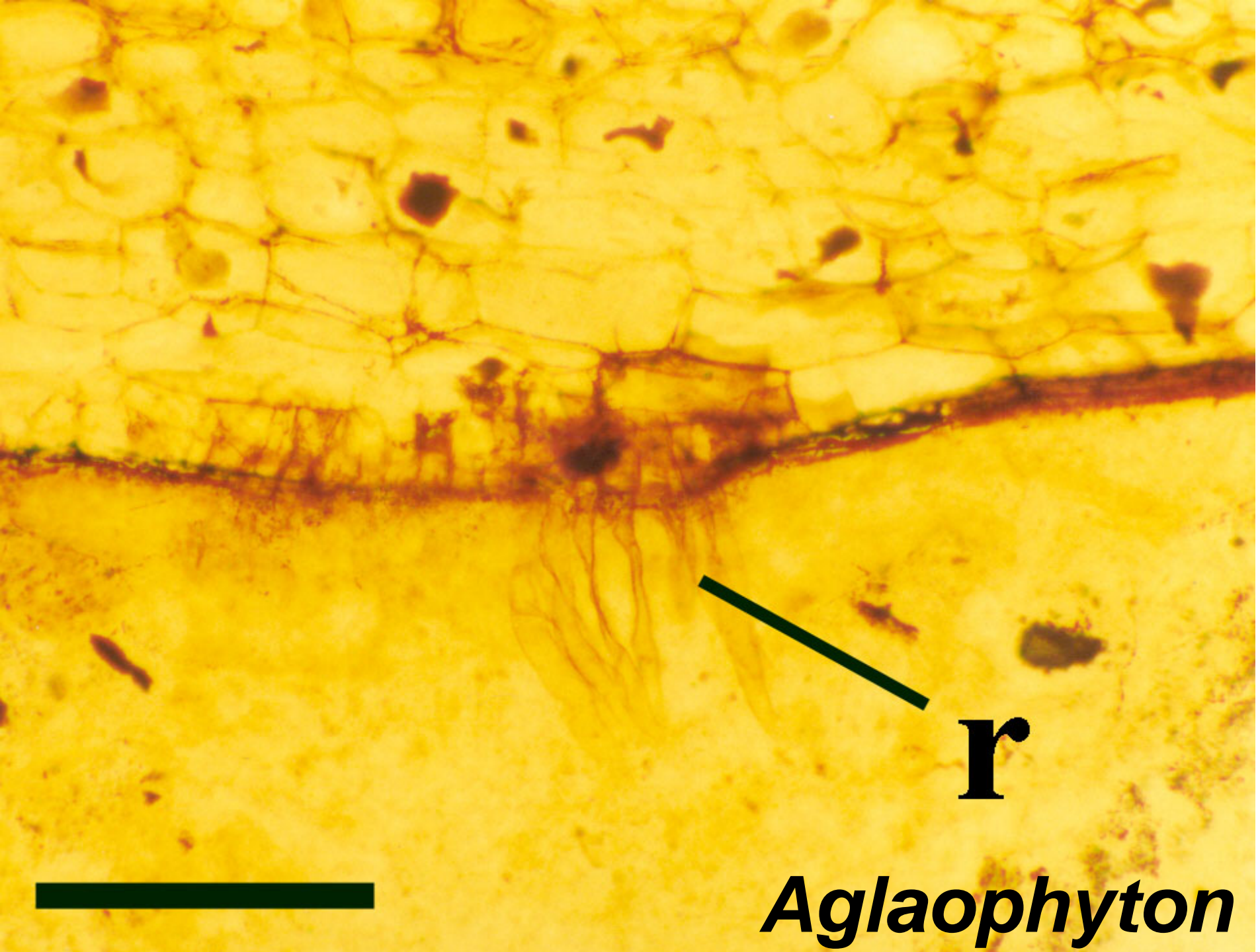


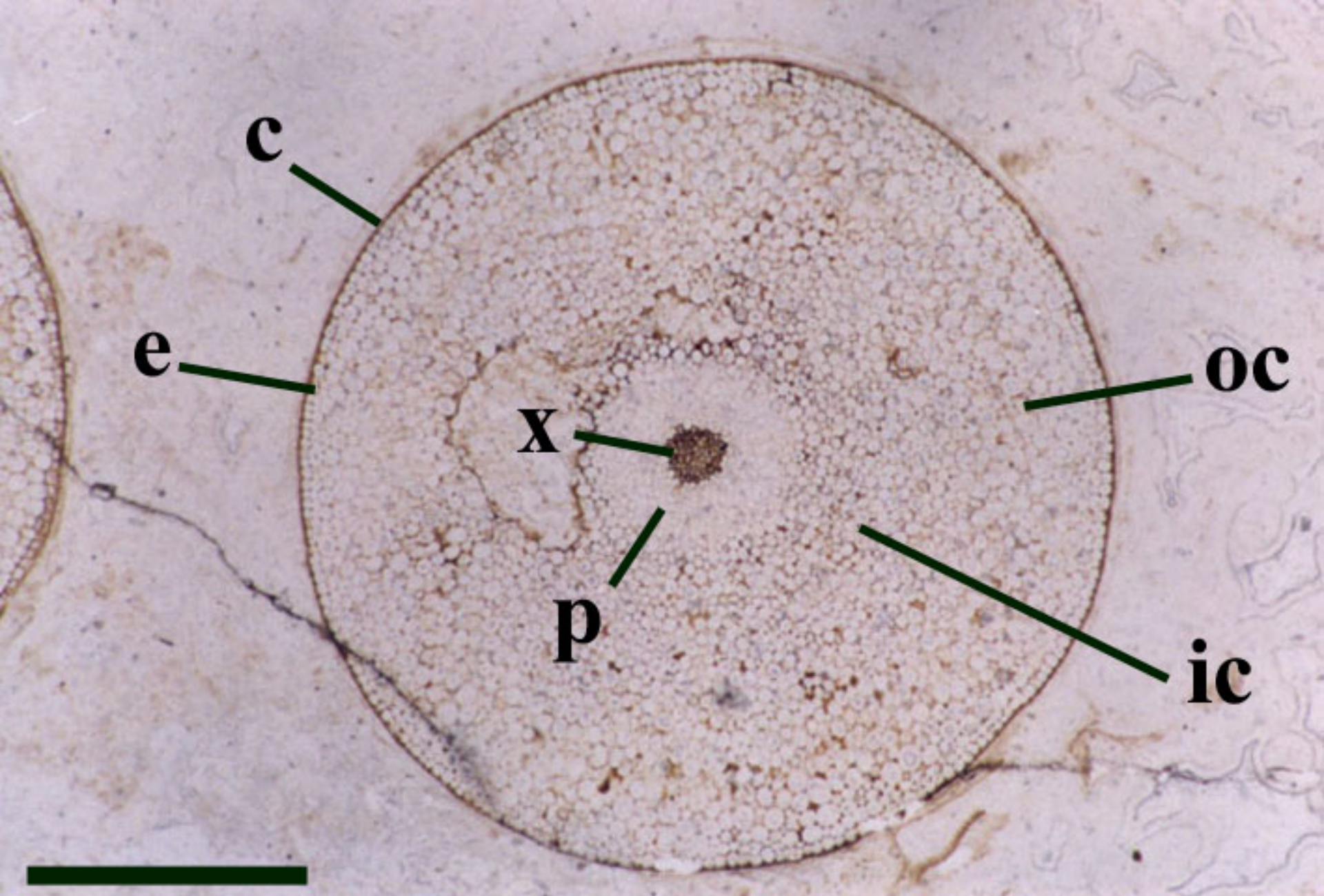


Aglaophyton

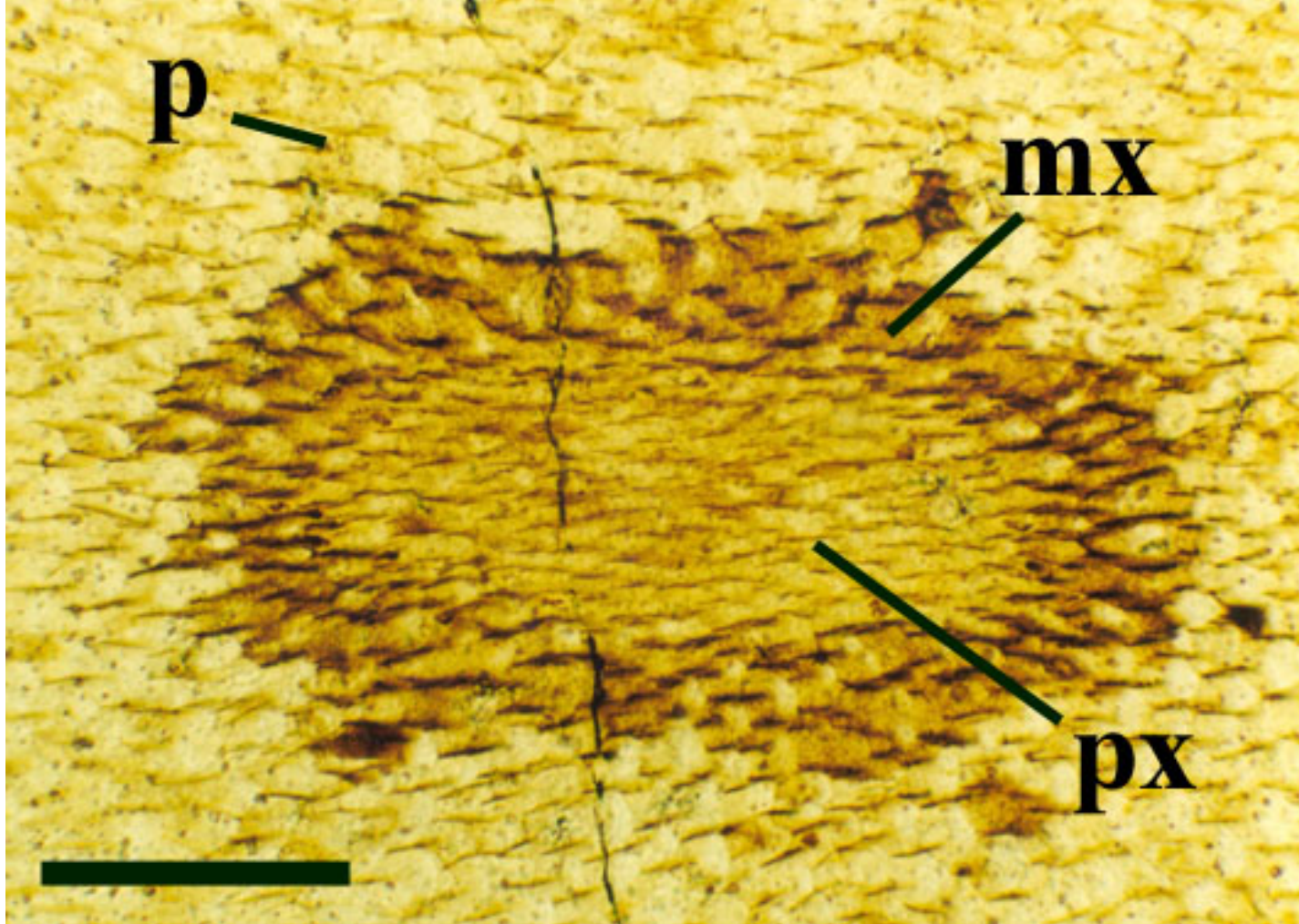


Aglaophyton

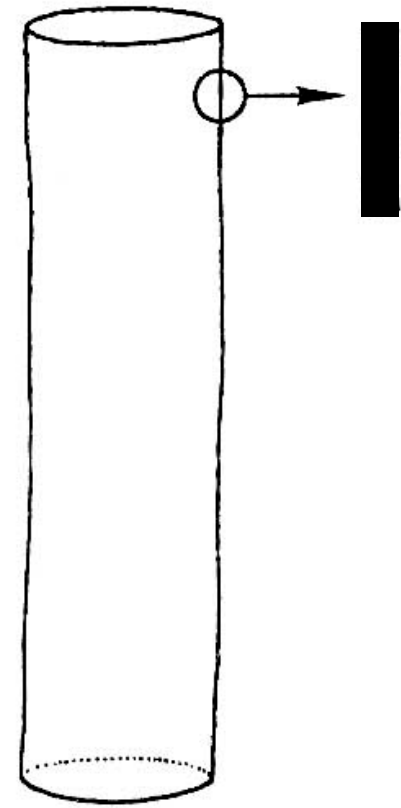
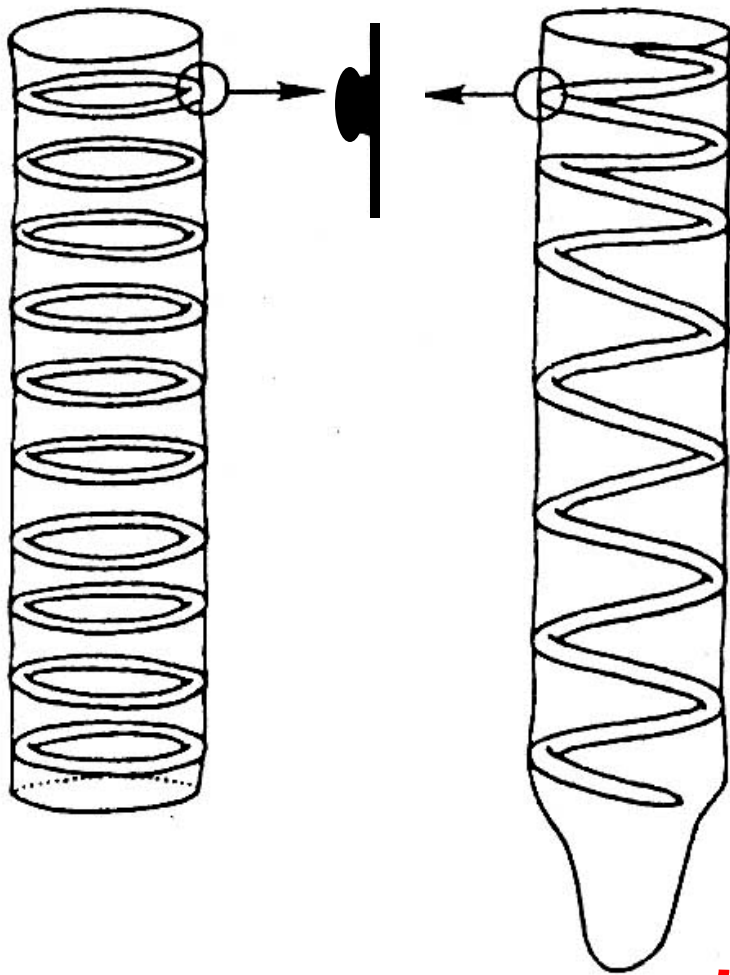




Aglaophyton

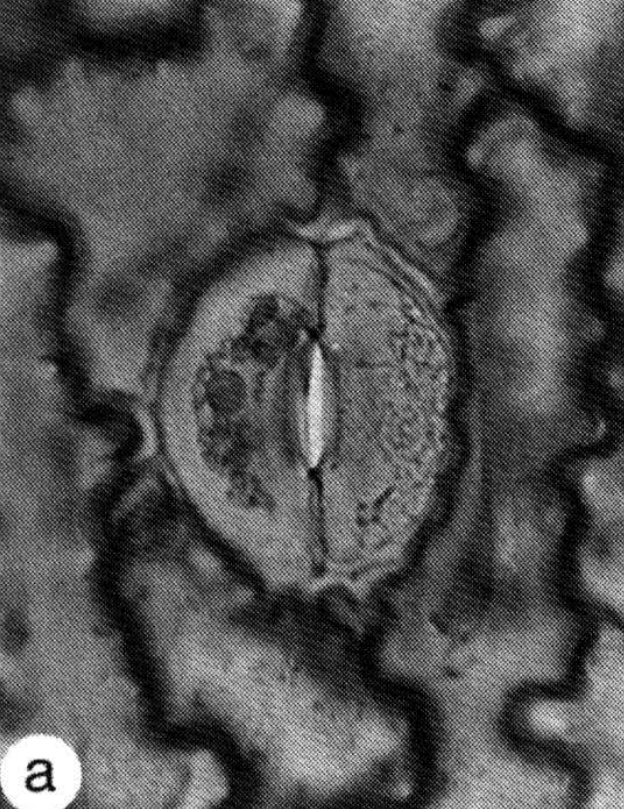


**Aglaophyton
major**



кольчатая и спиральная
трахеиды сосудистых растений

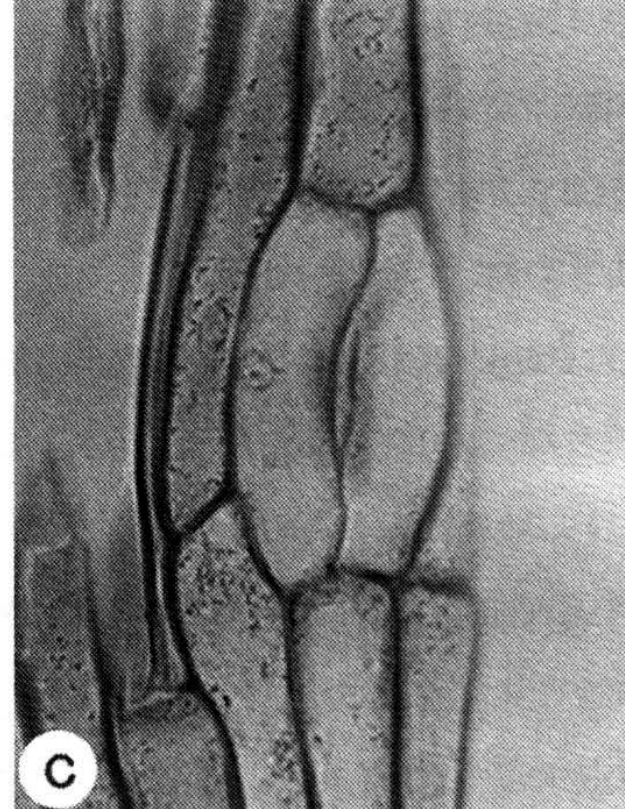
гидроиды мохообразных



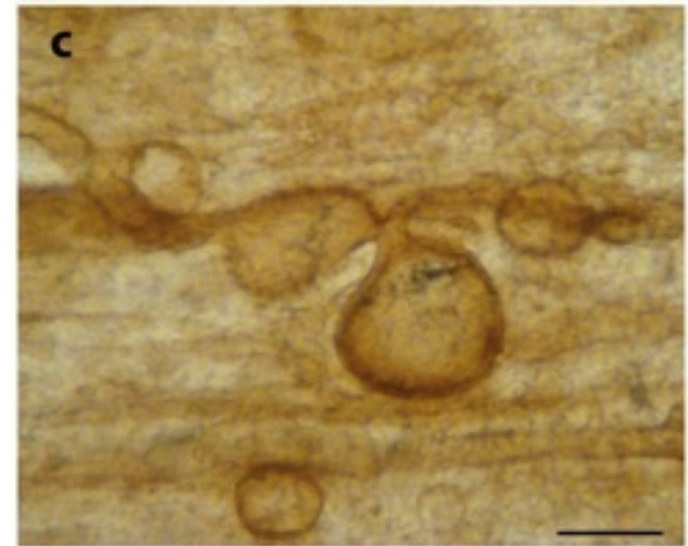
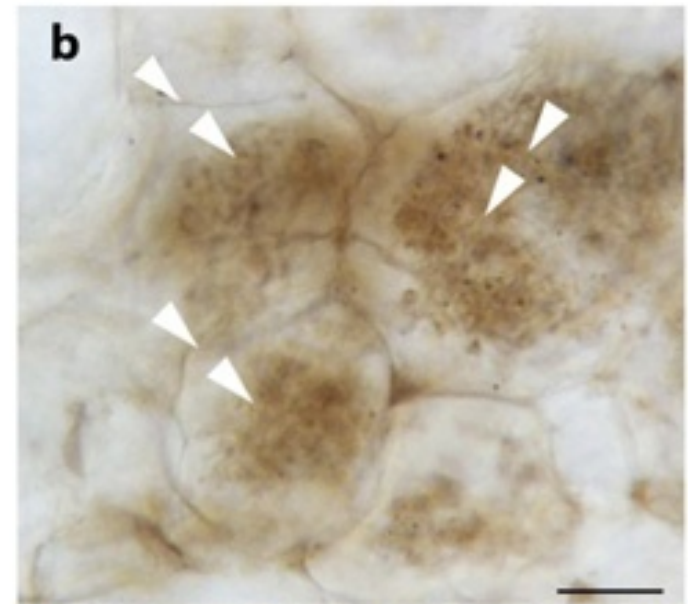
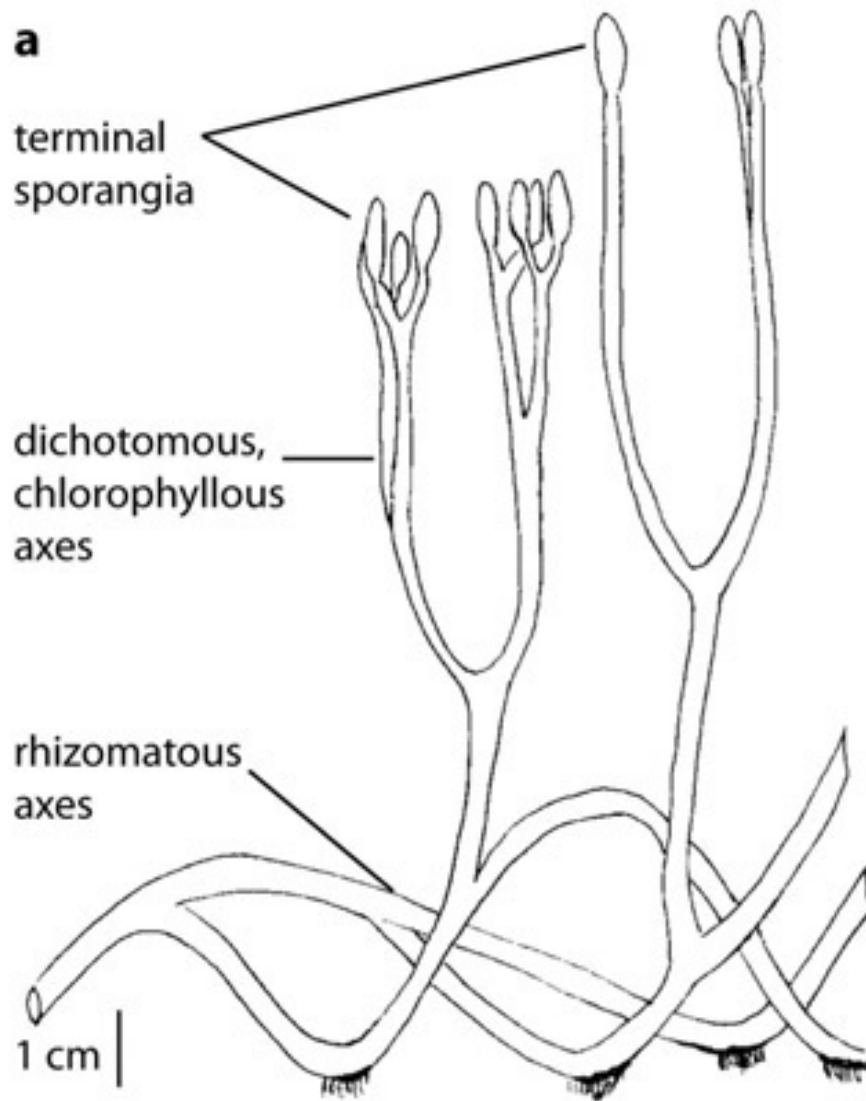
Lycopodium



Aglaophyton



Anthoceros

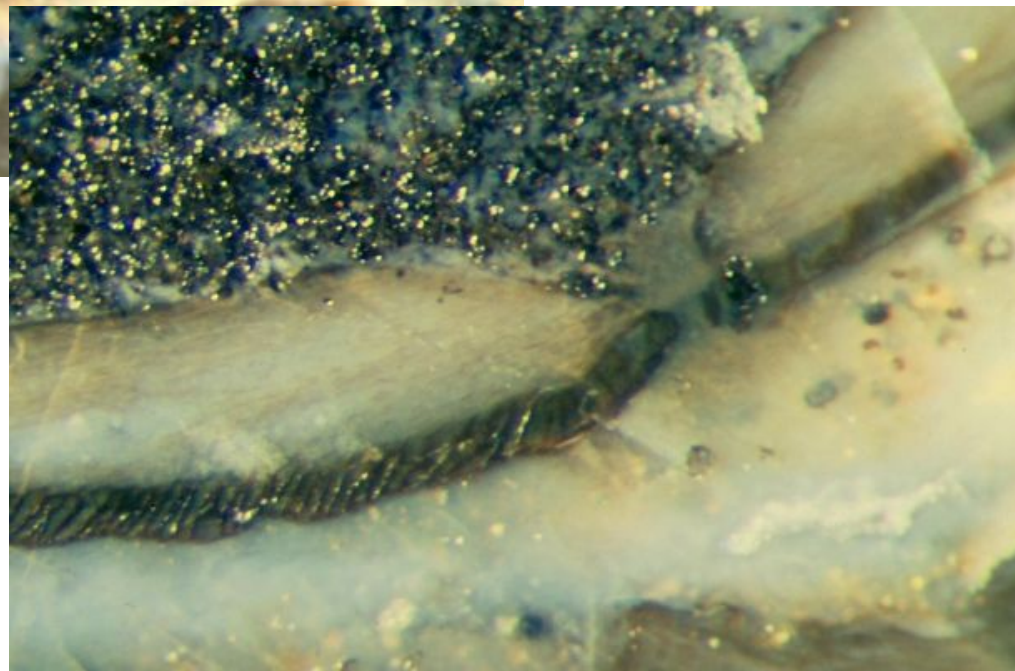
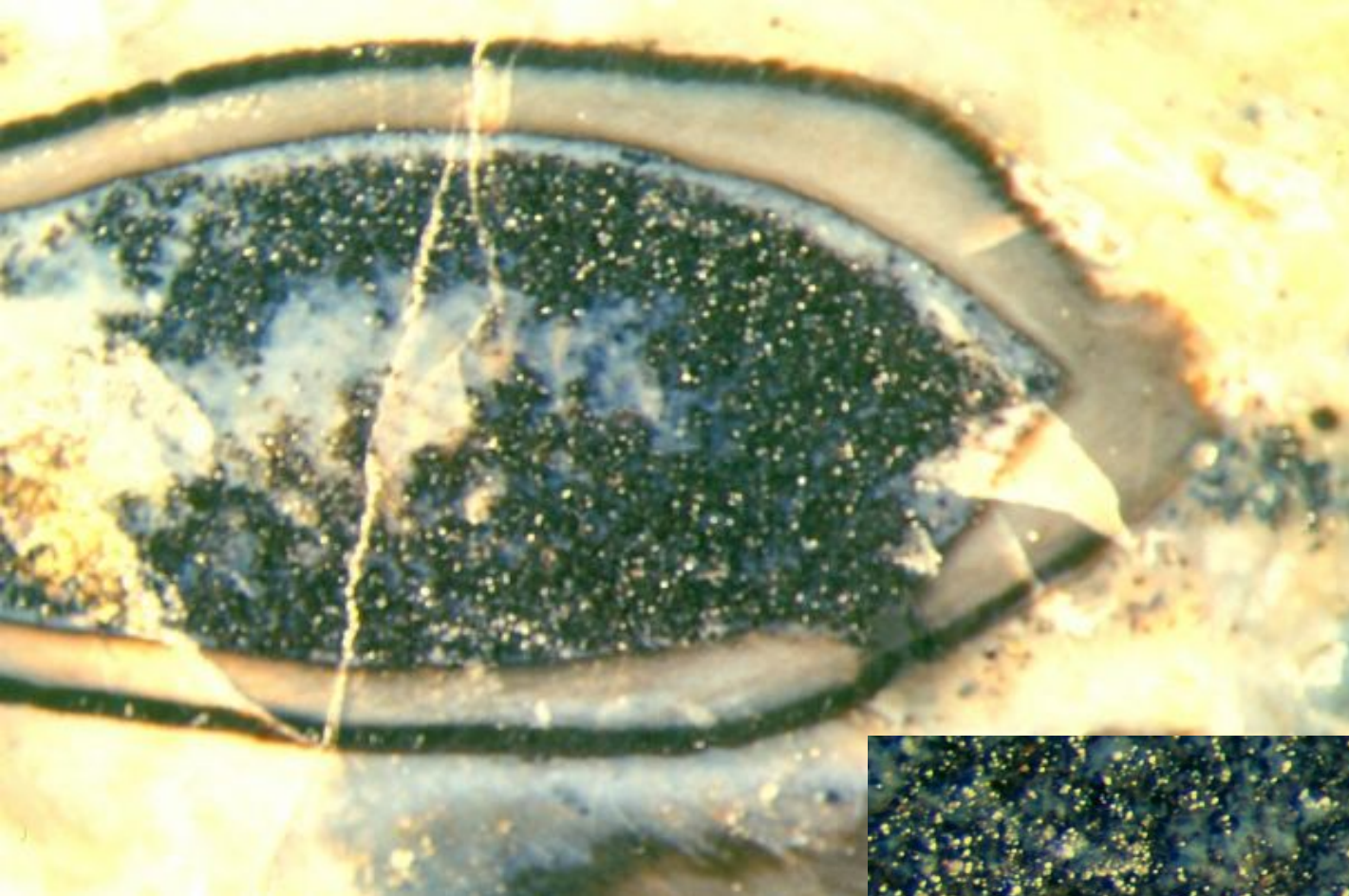


Arbuscular mycorrhizal colonization by Glomeromycetes (paramycorrhizae) in aerial and rhizomatous axes of the Rhynie chert plant *Aglaophyton major*. (a) General shape of the plant. (b) Colonized cortical cells of *A. major* showing intracellular arbuscules (white arrows) in turgid cells (photo courtesy of H. Kerp). (c) Hyphae and vesicles in the cortex of an aerial axis of *A. major* (photo C. Strullu-Derrien). Scale bars: (b) = 20 μ m; (c) = 40 μ m. **Selosse, Strullu-Derrien (2015).**



Aglaophyton:

Поперечный срез вскрывшегося спорангия с налегающими друг на друга краями

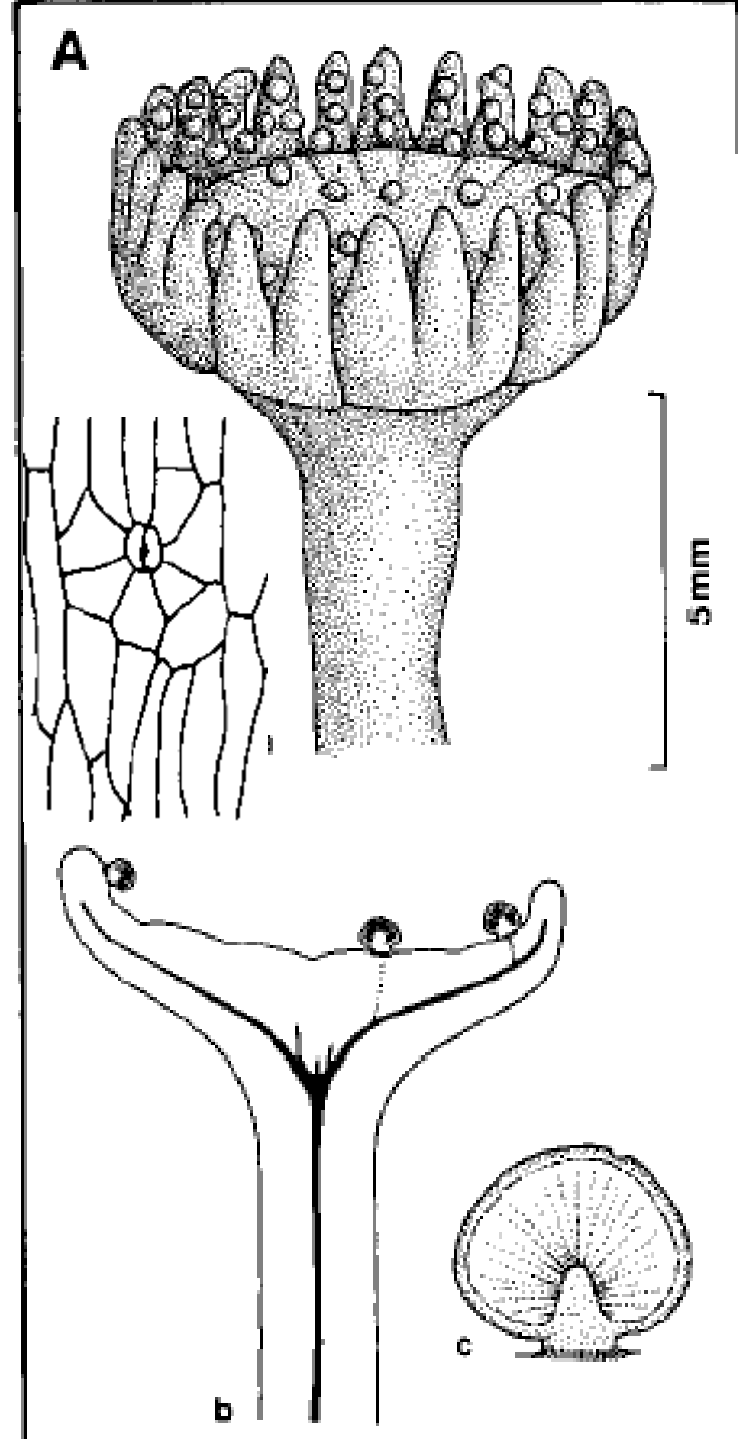


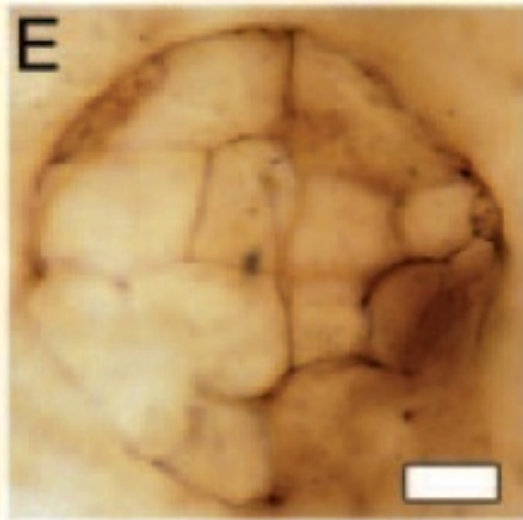
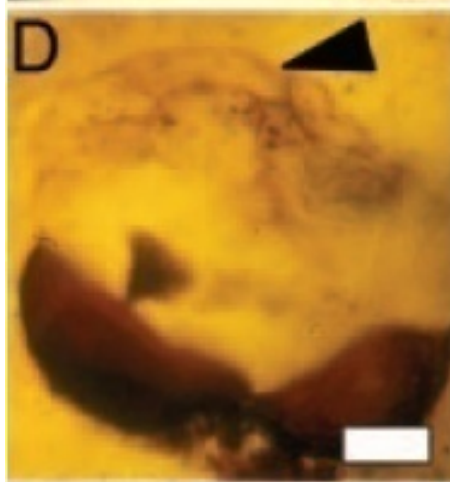
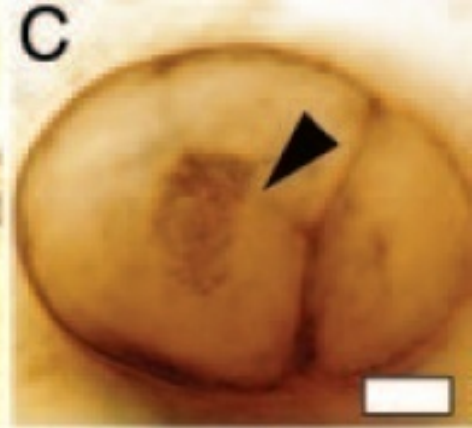
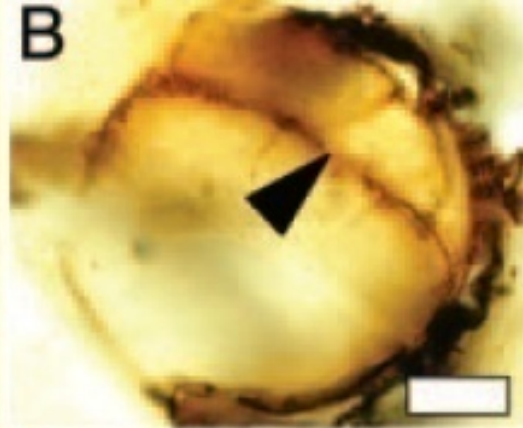
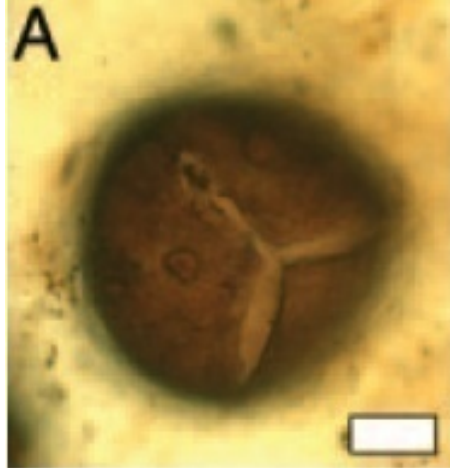
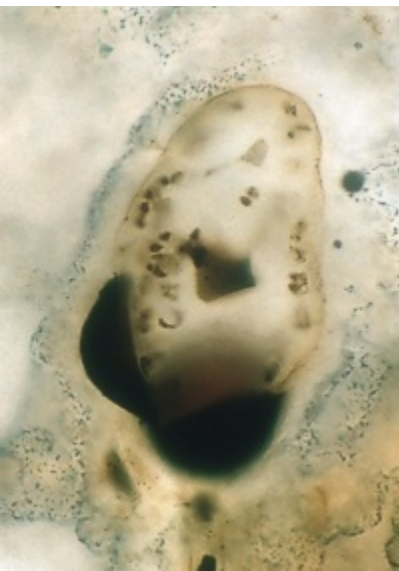
Aglaophyton:

Продольный срез спорангия с
отверстием, прогрызенным
неизвестным фитофагом

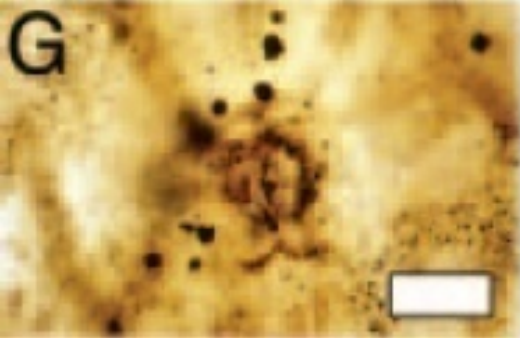


Lyonophyton rhyniensis





Lyonophyton = гаметофит *Aglaophyton*:
прорастание споры и ранние стадии
развития гаметофита

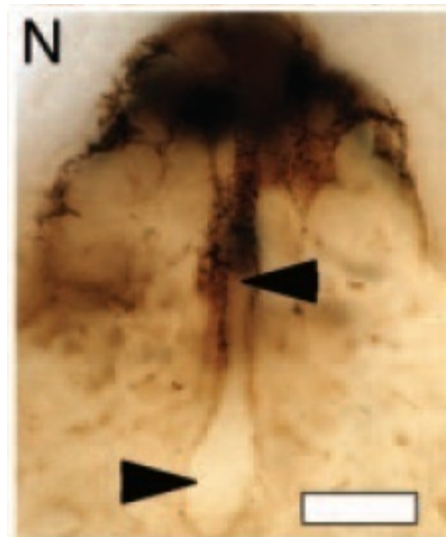


устье

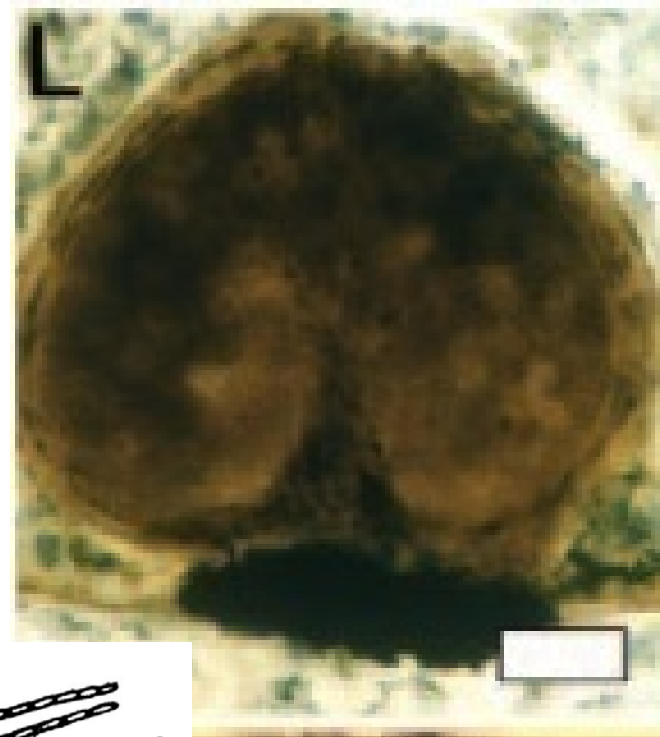


гифы гриба в паренхиме

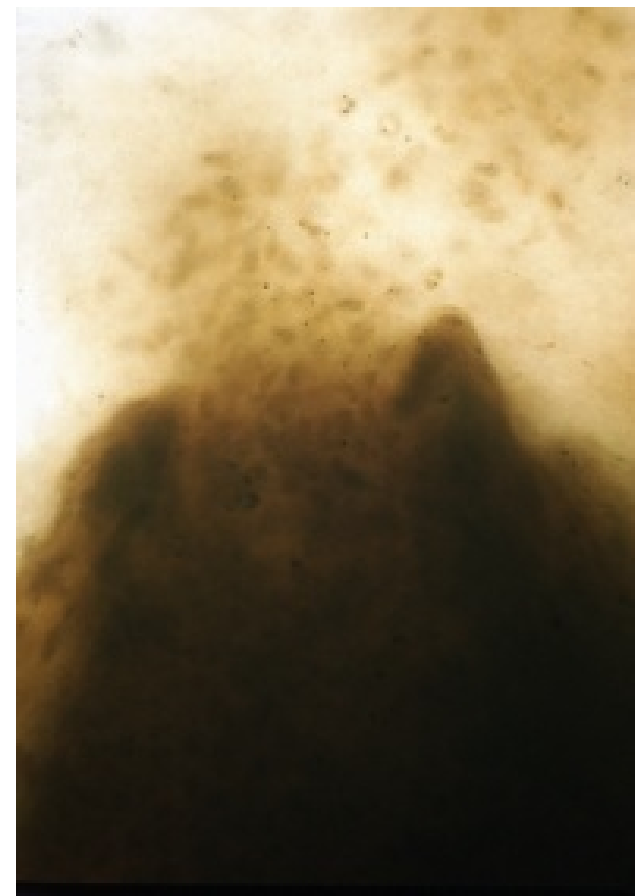
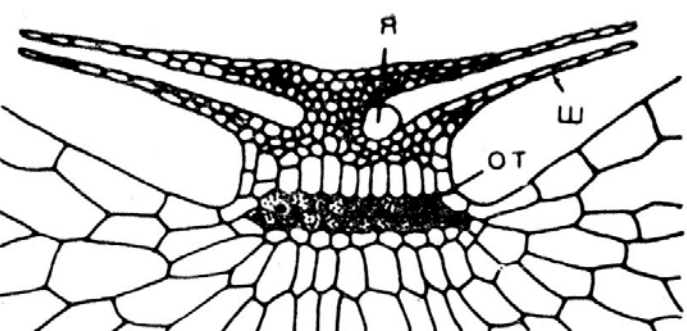
Lyonophyton
(= гаметофит
Aglaophyton)



архегоний



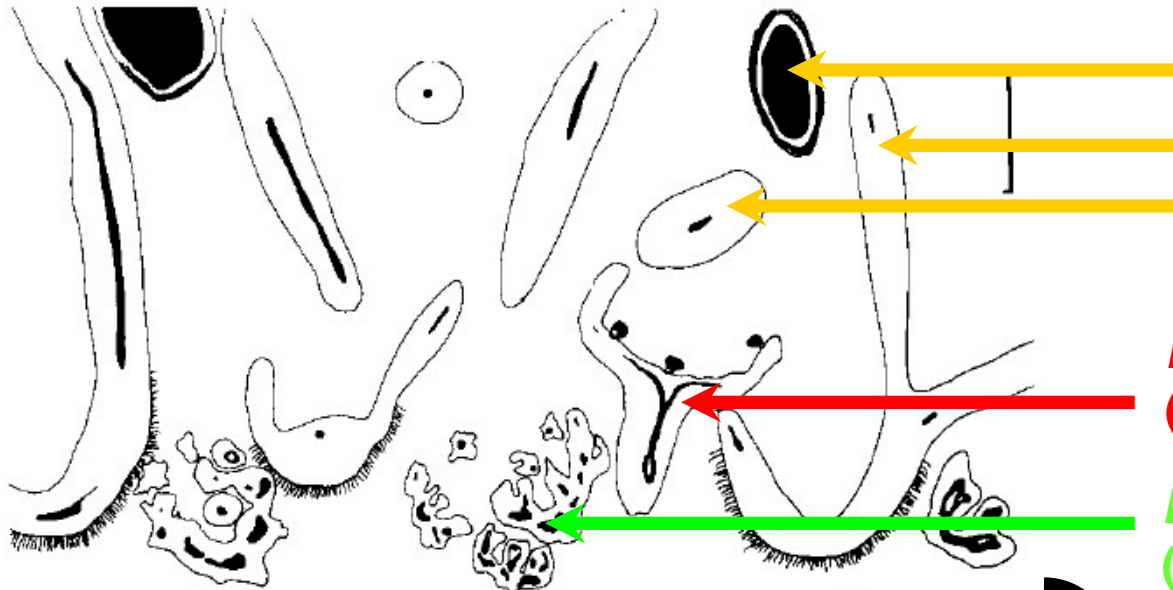
антеридий



выход сперматозоидов



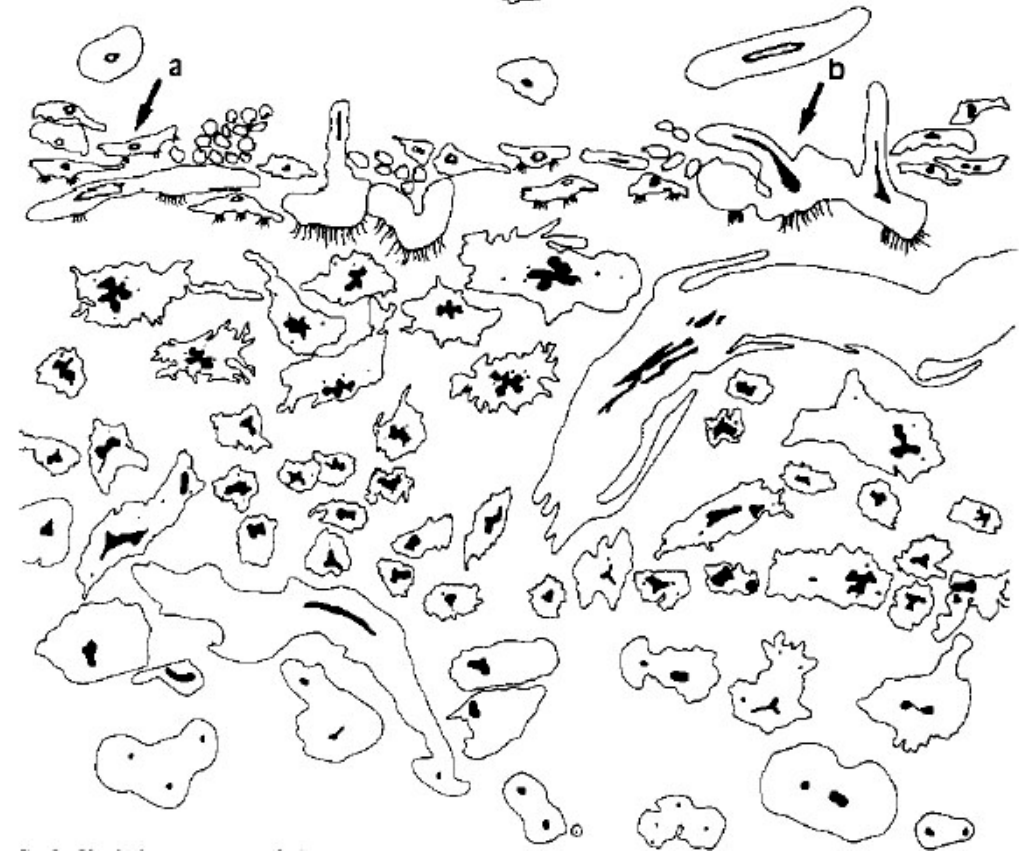
Fig. 1. Life history of *A. major*/*L. rhyniensis* showing stages in the development of the dimorphic gametophytes. The mature sporophyte (lower left) bears sporangia with spores of two types. Blue spores develop into mature antheridiophores; orange spores develop into archegoniophores.



Aglaophyton

Lyonophyton
(гаметофит *Aglaophyton*)

Langiophyton
(гаметофит *Horneophyton*)



отмершие остатки
Asteroxylon (древнейшее
плауновидное)